

Bifunctional Chelating Agents Based on Ionic Carbosilane Dendrons with DO3A at the Focal Point and Their Complexation Behavior with Copper(II)

Silvia Moreno,^{†,||} Paula Ortega,^{†,||} Francisco Javier de la Mata,^{†,||} Maria Francesca Ottaviani,^{*,‡} Michela Cangiotti,[‡] Alberto Fattori,[‡] María Ángeles Muñoz-Fernández,^{§,||} and Rafael Gómez^{*,†,||}

[†]Departamento de Química Orgánica e Inorgánica, Universidad de Alcalá, Edificio de Farmacia 28871, Alcalá de Henares, Spain

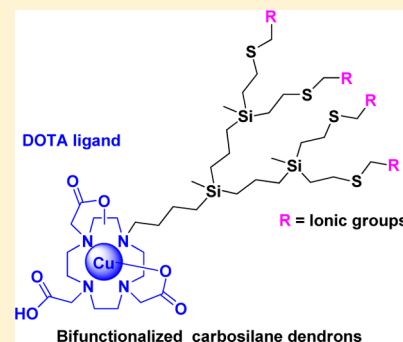
[‡]Departments of Earth, Life and Environment Sciences, University of Urbino, Via Ca' le Suore 2/4, Urbino 61029, Italy

[§]Laboratorio de Inmunobiología Molecular, Hospital General Universitario Gregorio Marañón, Madrid, Spain

^{||}Spain/Networking Research Center of Bioengineering, Biomaterials and Nanomedicine (CIBER-BBN), C/ Poeta Mariano Esquillor s/n 50018, Zaragoza, Spain

S Supporting Information

ABSTRACT: A synthetic protocol has been designed to incorporate the DO3A ligand to the focal point of cationic or anionic carbosilane dendrons, affording a set of bifunctional chelating agents (BFCAs) useful for potential biomedical applications. The complexation behavior study of ionic BFCAs has been accomplished by UV–vis and electron paramagnetic resonance spectroscopy as well as potentiometric titrations. The presence of the dendron branches modifies the complexation capacity of the macrocyclic ring with respect to that of the 1,4,7,10-tetraazacyclododecane-*N,N',N'',N'''*-tetraacetic acid (DOTA) ligand. Also, a different behavior has been observed in the carboxylate-terminated dendrons against analogous sulfonate- or amine-terminated dendrons in the contribution of the branches and peripheral groups to the coordination modes. The presence or not of Cu–S₂O₂ coordination sites and the generation can be important factors to take into account for considering a particular biomedical application.



INTRODUCTION

In the past, many metal complexes from acyclic and macrocyclic ligands have found important applications in diagnostic and therapeutic medicine, being nowadays an area of growing interest.^{1,2} All these metal ions need to be strongly coordinated with a suitable ligand to guarantee a safe administration *in vivo*. In this way, the inherent free metal ion toxicity is avoided. The DOTA (1,4,7,10-tetraazacyclododecane-*N,N',N'',N'''*-tetraacetic acid) ligand and its DO3A (1,4,7,10-tetraazacyclododecane-*N,N',N'',N'''*-triacetic acid) analogue are important chelators commonly used for biomedical applications as therapeutic radiopharmaceutical and/or MRI contrast agent.³ They are able to form complexes with a large number of metal ions with high thermodynamic stability and kinetic inertness.³ Although, there are particular cases that show moderate *in vivo* stability, such as the radio-Cu(II)DOTA complex, DOTA is still one of the most used chelators due to its commercial availability, FDA approval, and mild labeling conditions. Introduction of a reactive functional group into the macrocycle allows the preparation of the so-called bifunctional chelate agents (BFCAs) as a common way to label biomolecules such as antibodies or peptides among others. Most of them were obtained as activated esters of DOTA or DO3A and the subsequent reaction with an amino group.^{4–8}

However, the chelation chemistry of the DOTA and DO3A ligands can be also accomplished with nonradioactive metals. In this context, the apparently critical involvement of metal ions, particularly Fe(III) or Cu(II), in some neurodegenerative pathogenesis renders chelation therapy a sensible strategy to be explored with these systems.^{9,10}

On the other hand, dendrimers are ideally monodisperse and multivalent macromolecules of nanoscale size. These features make them especially appropriate for biomedical applications in their interaction with different cellular components or the delivery of bioactive molecules such as nucleic acids.^{11–13} In this sense, cationic dendrimers have been extensively used as nonviral vectors for delivering nucleic acids both in *in vitro* and *in vivo* experiments,^{14–17} as antibacterial agents,^{18–20} or as scavengers of amyloid plaques in neurodegenerative diseases.^{21,22} However, anionic dendrimers were applied as antiviral agents.^{23–25} Concerning DOTA or DO3A ligands, dendrimers have been mainly used as an alternative scaffold capable of carrying multiple chelating ligands (among them DOTA or DO3A) to incorporate radiopharmaceuticals at well-defined positions.^{26,27} A more versatile topology within the

Received: May 11, 2015

Published: September 11, 2015



dendritic structure is the so-called dendrons, where the surface can be decorated with the same ionic groups as spherical dendrimers, but the focal point can be functionalized with different groups by orthogonal chemistry.²⁸ Very few examples have been reported conjugating a DOTA or DO3A ligand at the focal point.²⁹ In this situation, one can keep the periphery for the desired biomedical application while adding a new function at the focal point, normally as a radiolabeling moiety.

In our group, spherical ionic carbosilane dendrimers have been extensively used in different biomedical applications.^{30–32} The biomedical information achieved in these previous studies may be transferred to carbosilane dendrons,^{33,34} which offer the possibility to prepare precise biofunctionalized systems with a double action. Here, we describe the synthesis and characterization (using NMR techniques and high-performance liquid chromatography–mass spectrometry, HPLC-MS) of cationic and anionic carbosilane dendrons conjugated with DO3A at the focal point and the evaluation of their coordination chemistry properties with Cu(II) as probe, in order to provide information for their use in biomedical applications. Characterization of Cu(II) complexes was achieved using potentiometric titration and electron paramagnetic resonance (EPR) and UV–vis spectroscopies. The EPR analysis has already been used to characterize the Cu(II) complexes of carbosilane dendrimers with sulfonated or carboxylated N-donor ligands^{35,36} as well as other types of dendrimers,^{37–39} providing detailed information on the coordination modes and the complex structures.

RESULTS AND DISCUSSION

The synthesis of a variety of ionic carbosilane dendrons with different peripheral functions (NMe₂, SO₃Na, and COONa) and DO3A at the focal point is described in the following:

DO3A Conjugated to Vinyl-Terminated Dendrons.

These dendrons were described from carbosilane vinyl dendrons BrG_nV_m of generations one (I) and two (II) with two and four terminal groups, respectively, which were previously described elsewhere.³³ The simplified structure and nomenclature of the starting materials are shown in Figure 1.

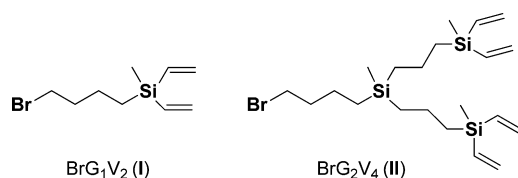


Figure 1. Structures of precursors based on carbosilane vinyl dendrons BrG_nV_m where *n* denotes the generation number and *m* is the number of peripheral units.

Dendrons with a protected DO3A ligand at the focal point were prepared by two subsequent substitution steps on the CYCLEN ligand. The first consists of the reaction of an excess of CYCLEN with dendrons I or II using soft conditions to facilitate the monosubstitution process, affording (CYCLEN)-G_nV_m (where *n* = 1, *m* = 2 (1); *n* = 2, *m* = 4 (2) (see Scheme 1). The reaction was followed by ¹H NMR through the disappearance of the CH₂Br signal at δ 3.40. The new chain Si(CH₂)₄N was confirmed by TOCSY ¹H NMR, which showed two multiplets for SiCH₂CH₂CH₂CH₂N and two triplets for SiCH₂CH₂CH₂CH₂N. The presence of the new CH₂N fragment was identified as one triplet at δ ~2.38 in the ¹H NMR spectra (see Figure 2A) and at δ ~54.1 in the ¹³C NMR spectra (see Figure S1 in the Supporting Information, SI). A set of resonances located in the range δ 2.35–2.75 was attributed to the methylene groups of the macrocyclic chelator. Furthermore, HSQC {¹H–¹⁵N} NMR spectroscopy showed two cross-peaks belonging to the nitrogen atoms NH and N-dendron at δ ~20.5 (br) and 28.7, respectively. HPLC-MS chromatography was performed from the crude product to quantify the percentages of monosubstitution, showing 80% of monosubstitution for generation 1 (see Figure 2B), and higher values for generation 2. The mixtures were nicely purified by size exclusion chromatography in THF to afford the dendrons 1 and 2 as colorless oils.

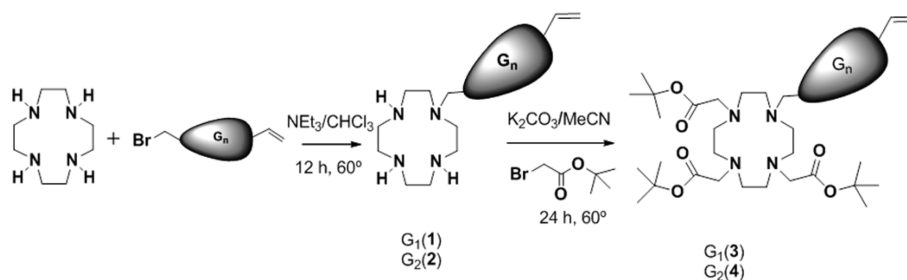
For the second substitution, *tert*-butylbromoacetate was used in acetonitrile as solvent at 60 °C for 24 h. The mixtures were purified again by size exclusion chromatography in THF to afford the dendrons [DO3A(O^{*t*}Bu)]₃G_nV_m (where *n* = 1, *m* = 2 (3); *n* = 2, *m* = 4 (4) (see Scheme 1) as colorless oils with high yields. The NMR data confirmed the incorporation of *tert*-butyl groups by the appearance of a peak at δ 1.44 in the ¹H NMR spectra and δ 28.2 in the ¹³C NMR spectra (see Figure S2 in the SI). However, the CH₂–N groups were observed as broad signals.

DO3A Conjugated to Ionic-Terminated Dendrons.

Systems 3 and 4 were treated with commercially available thiols under UV light to provide the functionalized dendrons in a 4 h reaction time. The obtained wedges were characterized by ¹H, ¹³C, and ²⁹Si NMR, as well as by elemental analysis and mass spectrometry when possible. The synthetic procedure is based on thiol–ene chemistry, a radical addition of the thiol derivative to the double-bond function of the peripheral dendron. The addition was regioselective at the β-position (*vide infra*). All the reactions were monitored by ¹H NMR, through the disappearance of the vinyl groups.

For the synthesis of carboxylate dendrons, the formation of previous ester units was needed. In this way, vinyl-terminated dendrons were treated with commercially available methyl thioglycolate to afford methyl acrylate-terminated structures

Scheme 1. Synthesis of Vinyl-Terminated Dendrons Containing CYCLEN (1, 2) or Protected DO3A (3, 4) at the Focal Point



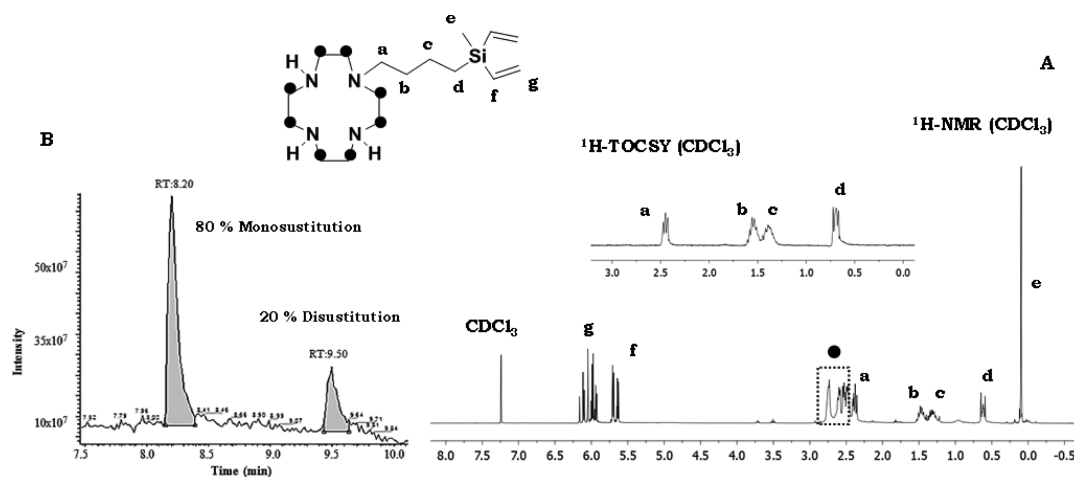
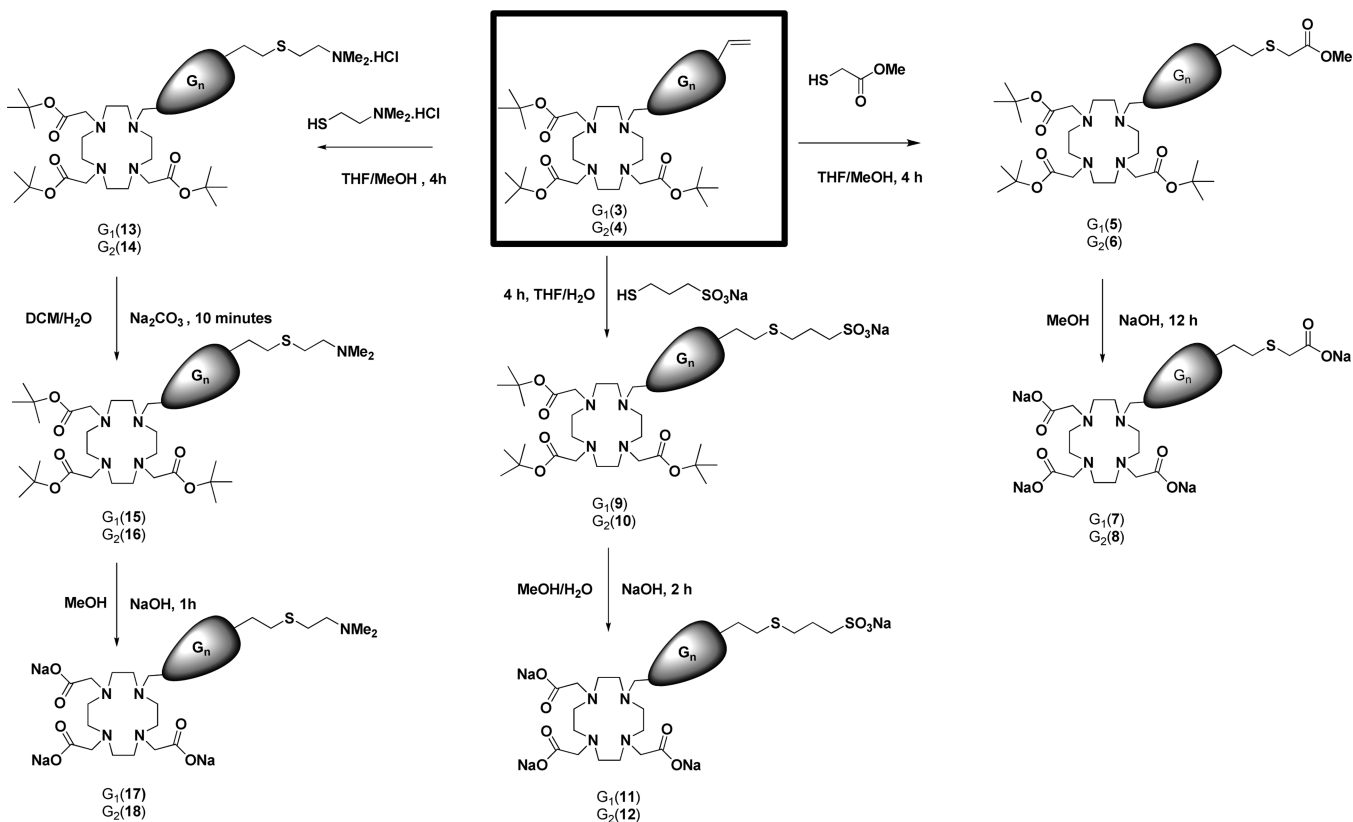


Figure 2. Spectroscopic and chromatographical data of dendron 1: (A) ^1H NMR and 1D ^1H TOCSY experiments; (B) HPLC-MS of the crude product.

Scheme 2. Synthesis of Neutral (Amine or Ester) and Ionic (Ammonium, Carboxylate, or Sulfonate)-Terminated Dendrons with Protected and Unprotected DO3A at the Focal Point^a



^aAll reactions were conducted at rt.

$[\text{DO3A}(\text{O}^t\text{Bu})_3]\text{G}_n(\text{COOMe})_m$ ($n = 1, m = 2$ (5); $n = 2, m = 4$ (6)) (see Scheme 2). The reactions were carried out in a solvent mixture of THF/MeOH under 365 nm UV light for 4 h and were purified by size exclusion chromatography in THF. Their ^1H NMR spectra presented two new peaks, one for the methylene group located between the sulfur atom and the carbonyl group SCH_2CO at $\delta \sim 3.22$ and another one as a result of the methyl ester located at $\delta \sim 3.71$ (see Figure 3A). In the ^{13}C NMR spectra, those groups appeared at $\delta \sim 33.0$ and 52.4, respectively, whereas the carbonyl group was located at δ 171

(see Figure S3 in the SI). The presence of the macrocyclic fragment was evidenced by the observation of two different $-\text{O}^t\text{Bu}$ groups at $\delta \sim 1.42$ in the ^1H NMR spectra.

Carboxylate-terminated dendrons were easily formed by the subsequent treatment of ester-terminated dendrons, 5 or 6, with sodium hydroxide in methanol overnight, giving rise to the anionic dendrons with unprotected DO3A at the focal point $[\text{DO3A}]\text{G}_n(\text{COONa})_m$ ($n = 1, m = 2$ (7); $n = 2, m = 4$ (8)) as yellow solids (see Scheme 2). Disappearance of the methyl ester and *tert*-butyl resonance in both ^1H and ^{13}C NMR spectra

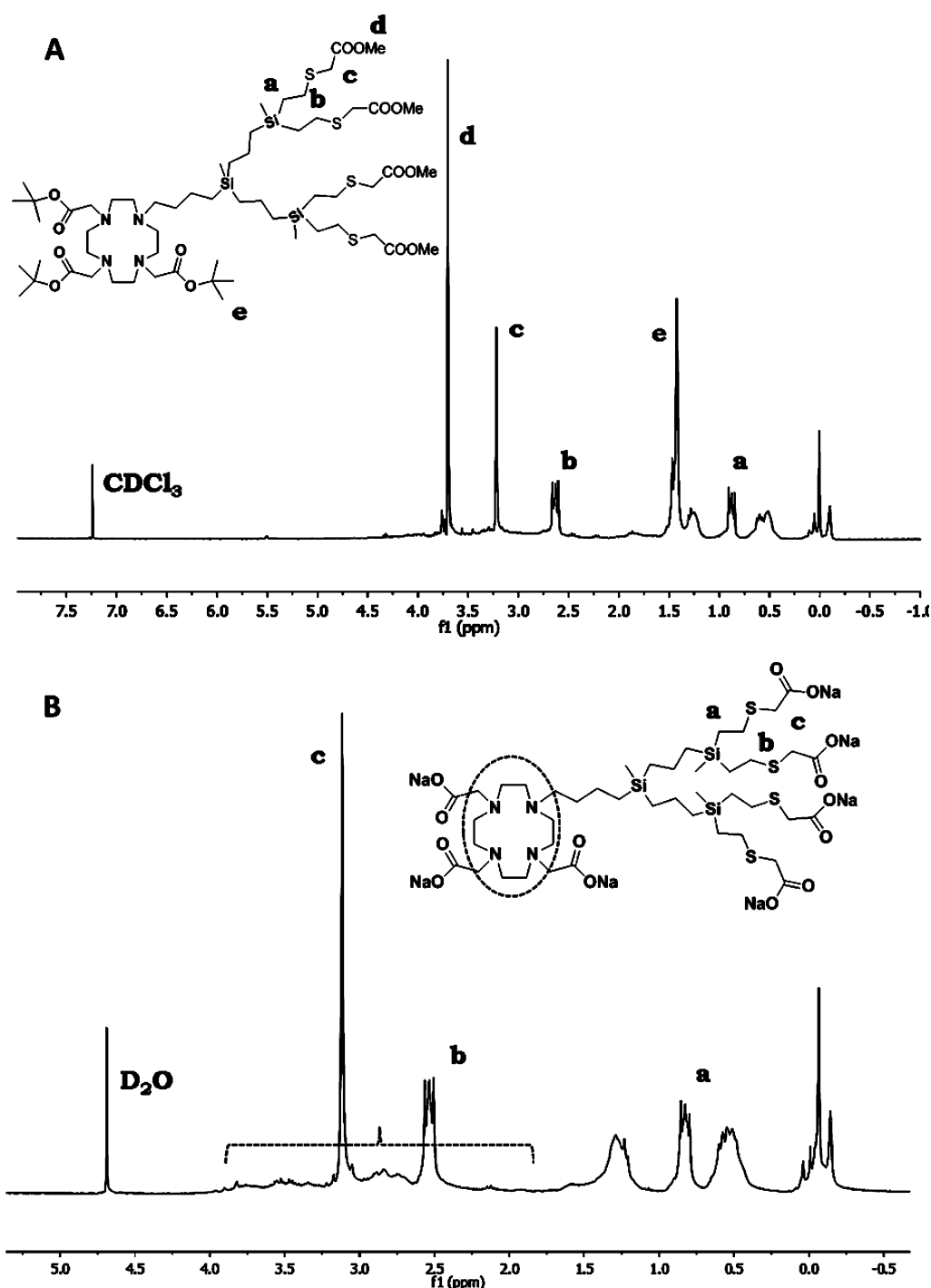


Figure 3. ^1H NMR spectra of dendron (A) $[\text{DO3A}(\text{O}^t\text{Bu})_3]\text{G}_2(\text{COOMe})_4$ (6) and (B) $[\text{DO3A}(\text{O}^t\text{Bu})_3]\text{G}_2(\text{COONa})_4$ (8).

confirmed the product formation (see Figures 3B and S4 in SI). The second generation was purified by dialysis (with molecular weight cutoff membranes $M_w = 500$), while the first generation was purified by a Sephadex column in water due to its smaller size. ^1H NMR spectra show one singlet around δ 3.12 for the methylene group bonded to the CO group and one multiplet located at δ 2.53 for the internal methylene bonded to the sulfur atom. In the ^{13}C NMR the COONa carboxylate carbon atom appeared at δ 178.8 shifted to lower field than the analogue methyl ester derivatives. The signals of the macrocyclic unit were overlapped by the dendritic structure.

In a similar synthetic procedure to the one described above (see Scheme 2), the addition of sodium 3-mercaptopropanesulfonate to the same double bonds of functionalized carbosilane dendrons 3 and 4, along with a photoinitiator (2,2-dimethoxy-2-phenylacetophenone, DMPA), in a solvent mixture of THF/ H_2O under 365 nm UV light for 4 h afforded the corresponding sulfonate-terminated structures $[\text{DO3A}(\text{O}^t\text{Bu})_3]\text{G}_n(\text{SO}_3\text{Na})_m$ ($n = 1, m = 2$ (9); $n = 2, m = 4$ (10)). After purification by dialysis ($\text{MWCO} = 500$ Da), dendron 10 was obtained in moderate yields as white-yellow solid. However, dendron 9, which has a poor water solubility, was purified in the next step. Analogously, in the ^1H NMR

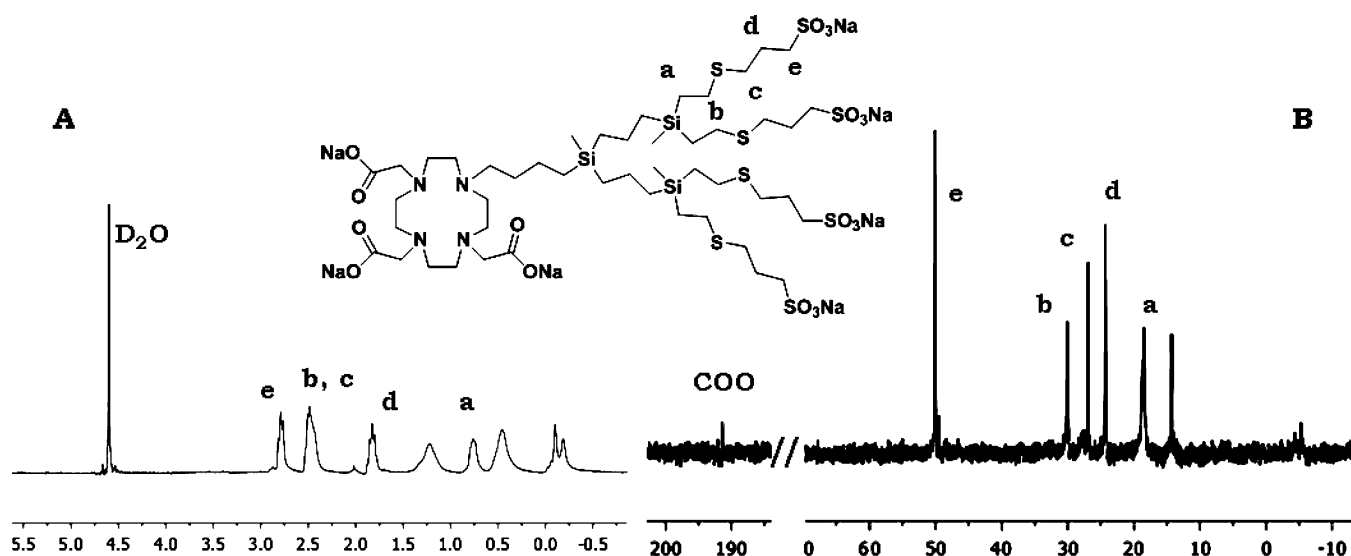


Figure 4. NMR data of dendron $[\text{DO3A}]G_2(\text{SO}_3\text{Na})_4$ (**12**): (A) ^1H NMR and (B) ^{13}C NMR spectra.

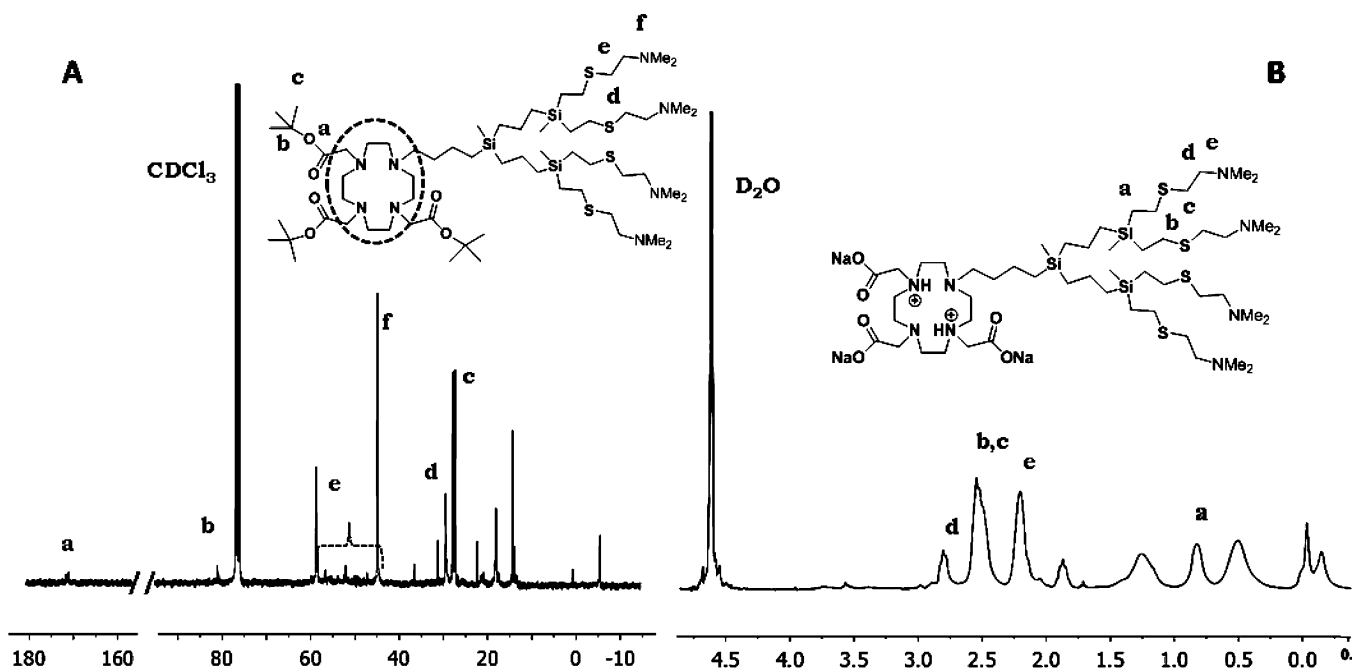


Figure 5. (A) ^{13}C NMR spectrum of dendron $[\text{DO3A}(\text{O}^t\text{Bu})_3]G_2(\text{NMe}_2)_4$ (**16**) and (B) ^1H NMR spectrum of dendron $[\text{DO3A}]G_2(\text{NMe}_2)_4$ (**18**).

spectra, a new chain of two methylene groups appeared at δ 2.58 and 0.87 after thiol–ene addition, and three new methylene groups at δ 2.84, 2.58, and 1.93 confirmed the presence of propanesulfonate units.

In order to obtain sulfonate-terminated dendrons with DO3A at the focal point, the deprotection of *tert*-butyl groups was performed by the treatment of dendrons **9** and **10** with sodium hydroxide in a mixture $\text{MeOH}/\text{H}_2\text{O}$ for 2 h, giving rise to the anionic dendrons $[\text{DO3A}]G_n(\text{SO}_3\text{Na})_m$ ($n = 1, m = 2$ (**11**); $n = 2, m = 4$ (**12**)) as yellow solids (Scheme 2). Disappearance of the *tert*-butyl resonance in both ^1H and ^{13}C NMR spectra along with the observation of a signal due to the carbonyl groups confirmed the product formation (see Figure 4). In these cases, purifications were also achieved by the same procedures as those used for the carboxylate analogues.

For ammonium-terminated dendrons, the precursors **3** and **4** were treated with commercially available 2-(dimethylamino)-ethanethiol hydrochloride. The reactions were performed in a mixture of solvents THF/methanol for 4 h of irradiation, in the presence of DMPA. The photoinitiator was added two times under deoxygenated conditions, to afford $[\text{DO3A}(\text{O}^t\text{Bu})_3]G_n(\text{NMe}_2\cdot\text{HCl})_m$ ($n = 1, m = 2$ (**13**); $n = 2, m = 4$ (**14**); see Scheme 2). All cationic dendrons were purified by dialysis (MWCO = 500 Da) and obtained as very hygroscopic white-yellow solids. The solids obtained were soluble in water and DMSO (see Scheme 2). The presence of the new chain $\text{Si}(\text{CH}_2)_2\text{S}$ was confirmed by ^1H NMR, which afforded two multiplets at δ 0.87 and 2.53 for the protons of the SiCH_2 and the CH_2S groups, respectively, whereas the outer chain $\text{S}(\text{CH}_2)_2\text{N}$ afforded two multiplets at δ 2.88 and 3.17 for the protons of the SCH_2 and the CH_2N groups, respectively.

Furthermore, a singlet at δ 2.71 confirmed the presence of the ammonium $-\text{NMe}_2\text{H}$ fragment. The ^{13}C NMR spectra confirmed the corresponding assignment from the ^1H NMR spectrum. The treatment of **13** and **14** with a Na_2CO_3 solution in a mixture of $\text{H}_2\text{O}/\text{CH}_2\text{Cl}_2$ (1:1) gave the neutral derivatives $[\text{DO3A}(\text{O}^t\text{Bu})_3]\text{G}_n(\text{NMe}_2)_m$ ($n = 1, m = 2$ (**15**); $n = 2, m = 4$ (**16**)) as pale yellow oils in high yields, soluble in organic solvents. The subsequent treatment with sodium hydroxide in a mixture of $\text{MeOH}/\text{H}_2\text{O}$ for 2 h led to dendrons $[\text{DO3A}]\text{G}_n(\text{NMe}_2)_m$ ($n = 1, m = 2$ (**17**); $n = 2, m = 4$ (**18**)). Again, disappearance of the *tert*-butyl resonance in both ^1H NMR spectra along with the observation of a signal due to the carbonyl groups confirmed the product formation (see Scheme 2, Figure S5, and the Experimental Section).

Study of Coordination Modes. Once these ionic systems were obtained, a study of their coordination modes was carried out through potentiometric titration and UV–vis and EPR spectroscopies, using Cu(II) as probe. Key factors influencing the stability of macrocycle-containing metal complexes based on DOTA or DO3A are related to cavity size, rigidity of the macrocycle backbone, and type, number, and position of pendant arms. Even a small change in the ligand structure can lead to a dramatic modification in the complex stability.⁴⁰ In addition, new coordination centers can be envisaged from the dendritic scaffold.

Potentiometric Titration of Dendrons. A potentiometric titration of the anionic- and amine-terminated dendrons of first-generation **7**, **11**, and **17** with DO3A at the focal point was performed in pure distilled water without ionic strength, and the experimental values of pK_a were measured by using the method of the second derivative (see the SI, Figures S5–S7) along with the theoretically calculated pK_a values of each group determined by the Marvin, Calculator Plugin, and Chemical Terms Demo.⁴¹ The compounds contain several basic centers in the dendritic structure, that is, the nitrogen atoms and the carboxylate groups of the DO3A moiety, the sulfur atoms of the branches, and the peripheral groups (carboxylate, sulfonate, or amine units). The pK_a values of sulfur atoms and the sulfonate groups are not observed, as expected, because they are too low to be determined by this technique. The titration curve of the amine-, sulfonated-, and carboxylate-terminated dendrons showed two pK_a regions with a pronounced difference between them (ca. 4.5 and 9.0), assigned to the acidic dissociation constants of the $[(\text{NH}^+) + \text{COOH}]$ and (NH^+) groups, respectively, and in agreement with the literature data.^{36,42} Although theoretical and observed data do not fit exactly, they indicate the same tendency with respect to the groups associated with the macrocycle. Therefore, in a pH range of 4–8, the sulfonate and carboxylate groups are in the anionic form and some of the macrocyclic N atoms found as amine groups, all of them prone to coordinate metal centers. In the case of amine-terminated dendrons, the protonatable N-donor units based on quaternized peripheral amines of the dendritic structure and some of the four nitrogens of the DO3A ligand would explain the water solubility observed by dendrons **17** and **18** and the lack of coordination at the periphery (*vide infra*). These features could be extended to all the second-generation dendrons.

pH measurements of the dendrons **12** and **18** in the presence of low concentrations of Cu(II) showed no significant changes in their values with respect to copper-free ligands, unlike what was observed for dendron **8**. These observations suggested selective coordination modes at the DO3A core for sulfonate-

Table 1. Comparative pH Measurements of Different Second-Generation Dendrons^a in the Presence of Cu(II)^b at Different Concentrations

ligand	pH values				
	copper free	0.01 M Cu(II)	0.05 M Cu(II)	0.1 M Cu(II)	0.3 M Cu(II)
DO3AG ₂ (COONa) ₄ (8)	10.26	8.97	7.36	^c	^c
DO3AG ₂ (SO ₃ Na) ₄ (12)	9.62	9.34	7.06	5.29	4.69
DO3AG ₂ (NMe ₂) ₄ (18)	8.64	8.07	6.91	5.55	5.20

^aLigand concentration (0.025 M). ^bCu(II) added as $\text{Cu}(\text{NO}_3)_2$.

^cPrecipitation.

or amine-terminated dendrons, while different possibilities of coordination can be inferred from the carboxylate-terminated dendrons. However, for high copper concentrations, pH values of dendron **8** were not obtained due to precipitation of the complex as a result of saturation (neutralization) starting of the peripheral coordination modes (see EPR data below). For dendrons **12** and **18** the pH values obtained at high Cu(II) concentrations were close to free $[\text{Cu}(\text{H}_2\text{O})_6]^{2+}$ or external Cu(II) complexes with a weak coordination strength. These results along with the solubility shown by these complexes even at Cu(II) concentrations above theoretical electroneutrality are in agreement with a low Cu(II) coordination at the periphery.

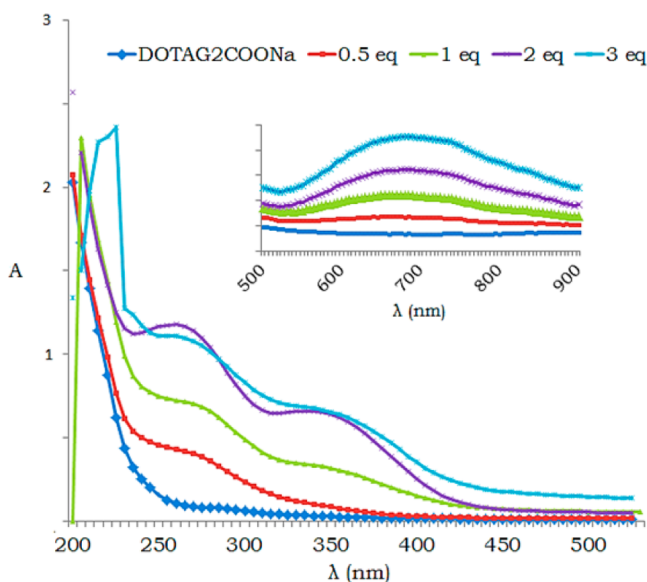
UV–Vis Characterization. Compounds **7**, **8**, **11**, **12**, **17**, and **18** were dissolved in pure distilled water at a concentration of 1 mM, and different equivalents of Cu(II) were added. The resulting complexes were diluted to a final concentration of 10^{-4} M for the UV–vis measurements (see Table 2). Figure 6 shows, as examples, the UV–vis spectra of dendron **8** with different equivalents of Cu(II) ($n = 0, 0.5, 1, 2, 3$).

The UV–vis spectra of carboxylate-terminated dendrons **7** and **8** at low Cu concentrations showed d–d transition bands around $\lambda_{\text{d-d}} = 700$ nm, far from the value observed for $[\text{Cu}(\text{H}_2\text{O})_6]^{2+}$ ($\lambda_{\text{d-d}} = 794$ nm) and therefore suggesting the presence of both O and N donor atoms in the coordination sphere. In addition, a tendency toward a trigonal bipyramid ($\lambda_{\text{d-d}} = 666\text{--}1000$ nm)^{43–45} or even pseudooctahedral^{46,47} environment can be inferred, instead of a square-base pyramid ($\lambda_{\text{d-d}} = 526\text{--}625$ nm). According to Prenesti et al.'s⁴⁸ model, it is possible to estimate the number and nature of the donor atoms bound to Cu(II). From the data obtained for compound **7** (the same can be deduced for dendrons **11** and **17**; see SI Table S.1) a N_4O_2 geometry can be inferred, where the axial groups of the octahedral environment may come from two N supporting carboxylic groups or one of them having the dendritic structure as substituent, ruling out again a square-base pyramidal geometry. Overlapped ligand to metal charge transfer (LMCT) bands from N and O donor atoms to Cu(II) ions were also present, in the range $\lambda_{\text{max}} = 250\text{--}300$ nm,^{35,49} indicating that at low Cu(II) concentrations, these metal ions are coordinated to the DO3A moieties and not at the periphery. However, on increasing the number of equivalents of Cu(II), a new LMCT attributed to sulfur–Cu interaction was observed at $\lambda_{\text{max}} = 350$ nm, confirming peripheral coordination modes. A more rigid structure with Cu(II) ions trapped through sulfur and oxygen atoms can be visualized.

Analogously, for sulfonate-terminated dendrons **11** and **12**, at low Cu(II) concentrations, the same bands as for **7** and **8** were observed, although, at higher Cu(II)/dendron molar ratios, LMCT attributed to sulfur atoms was not registered.

Table 2. UV–Vis Absorption (Maximum Values) of the Complexes Formed by Dendrons with Different Cu(II) Concentrations (Cu(II) Added as Cu(NO₃)₂)

dendron	Cu(II) equivalents	LMCT–MLCT	d–d transition
7	0.5	255	690
	1	250	670
	2	250, 330	685
	3	245, 330	690
	4	245, 330	690
8	0.5	270	
	1	270, 350	690
	2	260, 345	695
	3	265, 350	695
11	0.5	255	
	1	255	675
	2	255	680
	3	250	680
	4	250	680
12	0.5	245	660
	1	245	685
	2	245	700
	3	245	700
17	1	245	680
	2	245	685
	3	250	680
18	1	245	705
	2	245	680
	3	250	700
reference values	"CuO ₆ ": [Cu(OH ₂) ₆] ²⁺	200–300 nm	794 nm
	"CuN ₆ ": [Cu(NH ₃) ₆] ²⁺	200–300 nm	578 nm

**Figure 6.** Comparative UV–vis spectra of dendron 8 with different equivalents of Cu(II) ($n = 0, 0.5, 1, 2, 3$). A concentration of 0.1 mM was used as final dendron concentration. Cu(II) was added as Cu(NO₃)₂.

This observation indicates weak peripheral coordination without participation of heteroatoms in the coordination environment (see SI Figure S8).

In the case of the amine-terminated dendrons 17 and 18, the same UV–vis spectra are recorded as the sulfonate-terminated

dendrons (see SI Figure S9), both at low and high Cu(II) concentrations, as a consequence of protonation of terminal amines, which precluded peripheral coordination. All these features are in agreement with the different behavior observed in the potentiometric titration above-described and better clarified by means of the EPR analysis explained hereafter.

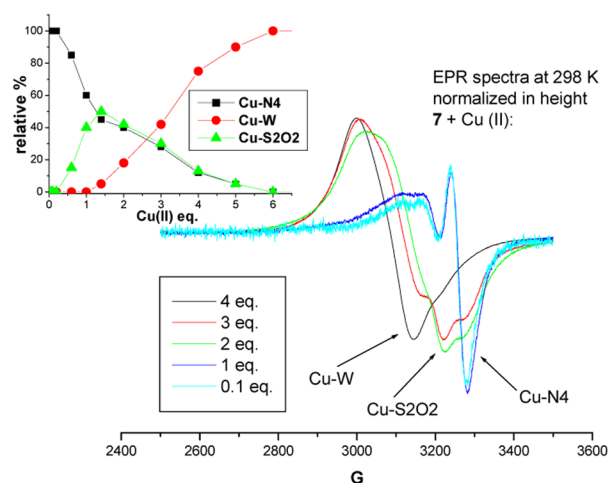
Finally, stability data for the complexation of 1 equiv of Cu(II) on DO3A–dendrons in solution in different conditions (time, temperature, and pH) have been obtained and based on the UV–vis spectra reproducibility (see SI Figures S10). No changes were observed for at least 2 weeks and below 50 °C for all dendrons. With respect to pH, the carboxylate-terminated dendrons are stable and in the range 4.5–8.5. However, for sulfonate-terminated dendrons decomposition begins to initiate at pH 8.5, being evident for amine-terminated dendrons at this value. These data must be considered by themselves a proof of the stability of these complexes, which is fundamental for their biomedical use.

EPR Characterization. EPR spectroscopy has been used to confirm the coordination modes of Cu(II) ions in these ionic carbosilane dendrons. The EPR spectra were obtained in water solutions at 298 and 150 K for all dendrons with different equivalents of Cu(II). Figure 7 exemplarily shows the experimental spectra (normalized in heights) obtained at 298 K for Cu(II) at various concentrations (expressed as equivalents of ions added to the dendrons at 0.1 M in surface groups) complexed by the first-generation dendrons DO3AG₁(COONa)₂ (7), DO3AG₁(SO₃Na)₂ (11), and DO3AG₁(NMe₂)₂ (17). Similar spectra were obtained using second-generation dendrons (see the SI, Figures S15, S17, S19).

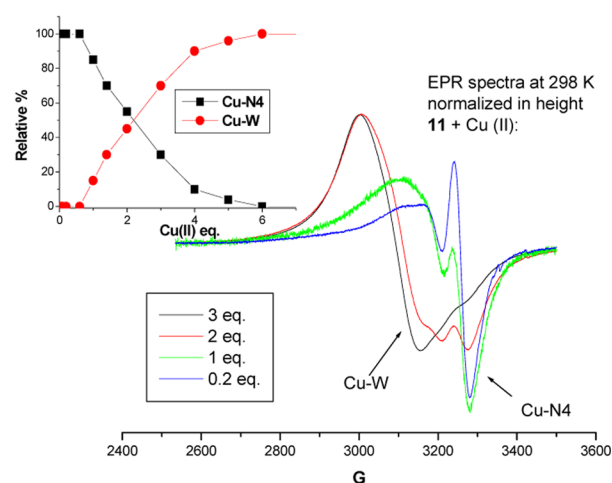
In several cases, the spectra were constituted by two or more components arising from different Cu(II) coordinations. These components were extracted by using a subtraction procedure between experimental spectra showing the same signals at different relative percentages. This subtraction procedure enabled the calculation of the relative percentages of the spectral components, which quantify the partitioning of the ions in different coordination structures. In Figure 7A–C the arrows indicate the main components constituting the spectra. At the highest Cu(II) concentrations, the spectra were apparently constituted by a single component, which was equivalent to the one found for Cu(II) free in water in the absence of the dendrons and the ligands. This signal was henceforth indicated as Cu–W, where W stands for water. Conversely, the first Cu(II) coordination sites which were occupied at the lowest Cu(II) concentrations were the nitrogen sites from the DO3A core. This coordination and the corresponding EPR signal are henceforth indicated as Cu–N₄. This coordination was identified by computing (program by Budil and Freed)⁵⁰ the spectra at the lowest Cu(II) concentrations, that is, below 1 equiv of Cu(II) and at both room (298 K) and low (150 K) temperatures (see SI Figures S11–S19).

Similarly, various components extracted from the subtraction procedure were computed, and these computations are also shown in the SI (Figures S11–S19). The main parameters extracted from computations (Table 3) were (a) the g_{ii} components (accuracy in the third decimal, on the basis of the computation itself) for the coupling between the electron spin and the magnetic field; (b) the A_{zz} component (accuracy of ± 0.5 G) for the coupling between the electron spin and the copper nuclear spin ($I_{Cu} = 3/2$); the g_{ii} and A_{zz} parameters

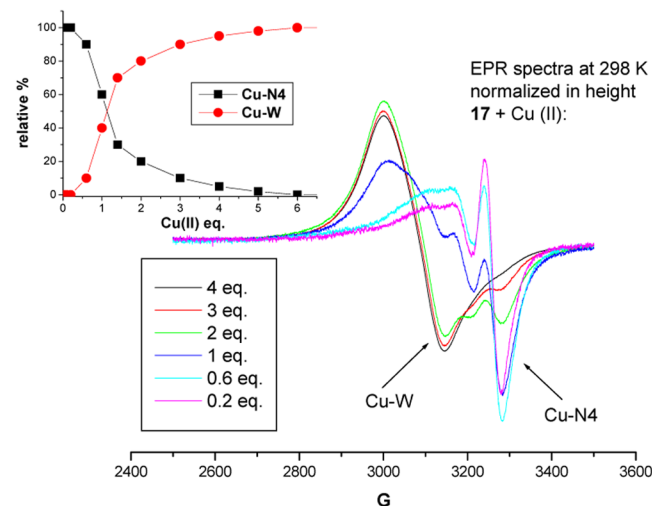
A



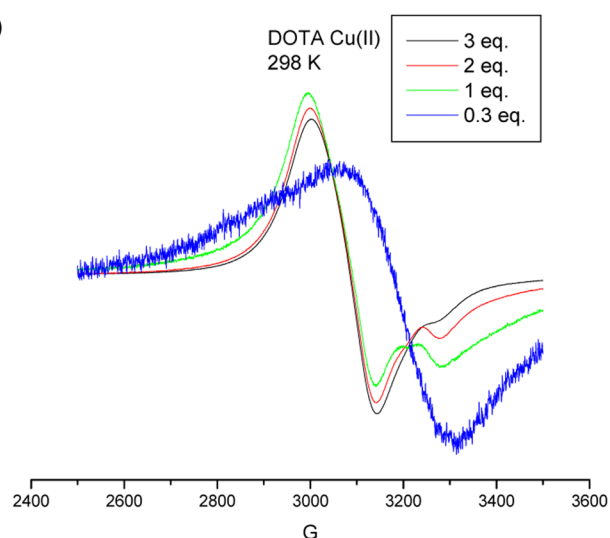
B



C



D



E

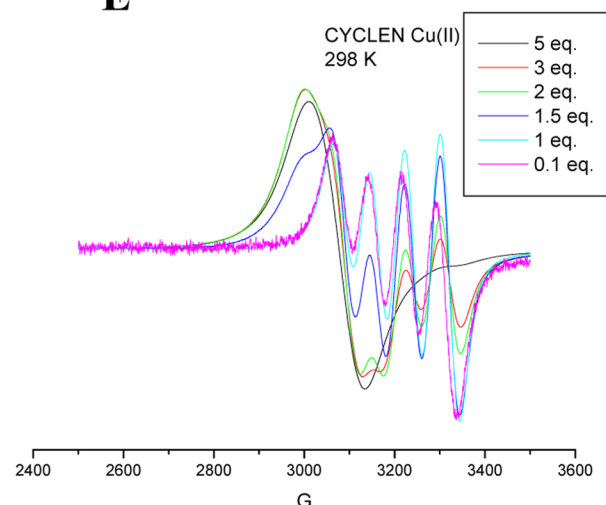


Figure 7. EPR spectra at 298 K (normalized in heights) of Cu(II) (from cupric nitrate salt) at various concentrations (expressed as equivalents of ions added to the dendrons) complexed by the G_1 dendrons (0.1 M in surface groups) in water solutions: (A) DO3AG₁(COONa)₂ (7); (B) DO3AG₁(SO₃Na)₂ (11); (C) DO3AG₁(NMe₂)₂ (17). The insets beside the spectra show the variation of the relative percentages of the spectral components as a function of Cu(II) equivalents. As references, selected EPR spectra of Cu(II) with DOTA (D) and CYCLEN (E) are also reported.

Table 3. Main Parameters Extracted from Computations of Cu(II) with Different Ligands Measured at 298 and 150 K

ligand	[Cu ²⁺] equiv	%	g_{xx}	g_{yy}	g_{zz}	$A_{zz}(\times 10^{-4} \text{ cm}^{-1})$	τ (ns)	coord
water	all	100	2.055	2.090	2.400	133.9	0.006	Cu–O ₄
CYCLEN	<1	100	2.005	2.043	2.190	178.9	0.02	Cu–N ₄
DOTA	<0.5	100	2.030	2.090	2.280	145.8	0.17	Cu–N ₂ O ₂ Cu–N ₄ O ₂
7	<1	100	2.013	2.048	2.253	172.5	0.23	Cu–N ₄
	2	42	2.051	2.141	2.393	137.4	2.00	Cu–S ₂ O ₂
8	<2	100	2.015	2.042	2.254	171.5	0.30	Cu–N ₄
	4	55	2.051	2.141	2.393	137.4	2.00	Cu–S ₂ O ₂
11	<1	100	2.013	2.044	2.253	172.5	0.2	Cu–N ₄
	1	85	2.020	2.055	2.260	169.9	0.28	Cu–N ₄
12	<0.25	100	2.007	2.030	2.239	180.8	3.32	Cu–N ₄
	0.25–1	100–80	2.015	2.042	2.253	171.5	0.30	Cu–N ₄
17	<0.6	100	2.010	2.050	2.250	174.4	0.2	Cu–N ₄
18	0.6	100	2.020	2.062	2.260	168.8	1.87	Cu–N ₄

indicate the coordination and structure of the Cu(II) complexes by using some selected references reporting on similar coordinations;^{35–39,51–54} (c) the correlation time for the diffusion rotational motion of the complexed Cu(II) ions, τ , which reports on the flexibility of the complex structure.

From the spectra reported in Figure 7 for G₁-dendrons + Cu(II) at 298 K, we found that DO3AG₁(NMe₂)₂ (17) (Figure 7C) and DO3AG₁(SO₃Na)₂ (11) (Figure 7B) show only the Cu–N₄ and Cu–W components, where the latter gains in relative percentage at the expense of the former by increasing the number of Cu(II) equivalents (see the insets in Figure 7B,C). Conversely, in agreement with UV–vis results, DO3AG₁(COONa)₂ (7) shows a further component whose relative percentage reaches a maximum between 1 and 2 Cu(II) equivalents (see the inset in Figure 7A). This component, also computed at room and low temperature (see Figure S14 in the SI), was identified as Cu(II) ions interacting with the sulfur sites and oxygen sites (Cu–S₂O₂) on the basis of previous literature.^{36,51–56} Ogawa et al.⁵⁵ have compared the EPR data from Cu(II) complexes with ethylthioacetate, propylthioacetate, and isopropylthioacetate. The first two ligands form a five-membered chelate ring, while isopropylthioacetate more likely forms a square-planar complex, like the cupric sulfate pentahydrate analyzed by EPR by Kneubuhl.⁵⁶ The dendron 7-Cu(II) system also shows a Cu–S₂O₂ square-planar structure, as indicated by the magnetic parameters. The oxygen sites in this complex may come from both carboxylate groups and water molecules. Previous studies on PPI dendrimers decorated with carboxylate and sulfonate groups³⁶ already showed that sulfonate groups are less interacting than the carboxylate ones.

Although in the solid state it is well known that the crystal structure of DOTA–Cu(II) reveals a monodentate coordination of two carboxylate groups to Cu(II),⁵⁷ in solution it is still unclear the role of the carboxylate groups at the DOTA or DO3A core regarding their participation in the complexation process. To answer this question, it is necessary to examine the spectra of DOTA and CYCLEN shown in Figure 7D and E, respectively. Surprisingly, these spectra, in both cases, are completely different from those of the dendrons at Cu(II) concentrations of <1 equiv. In more detail, the spectral computations in the SI (see Figures S11–S19) and the corresponding parameters in Table 3 indicated that the Cu(II)–CYCLEN and the Cu(II)–DOTA complexes have a stronger and a weaker Cu–N bond, respectively, compared to those in the Cu(II)–dendron complexes. This means that, due to the different line shapes, it is not possible to calculate the

EPR spectra obtained for the Cu(II) complexes formed with DO3A-linked dendrons by using the spectra of species formed with water, CYCLEN, and DOTA only. The strong Cu–N binding in the CYCLEN complex is also accompanied by a poorly distorted square-planar Cu–N₄ coordination and a fast motion at room temperature. Conversely, the weak Cu–N binding in the DOTA complex is due to the binding with the charged carboxylate groups attached at the macrocyclic ring as in the solid state. The parameters extracted from computation (Table 3) for the DOTA complex in solution indicate a Cu–N₂(COO)₂ coordination or an axially compressed octahedral structure Cu–N₄–(COO)₂, where the carboxylate groups occupy the axial positions, the latter being in agreement with the solid-state structure. The dendron branches attached at the DOTA core therefore modify the complexation behavior of the DOTA group toward Cu(II) by weakening the Cu(II)–COO binding and therefore strengthening Cu–N₄ binding.

The saturation of the dendritic binding sites by Cu(II) and the consequent appearance of the Cu–W complex are a useful manner to quantitatively characterize the complexation behavior of the dendrons in a comparative way. Figure 8 compares the variations of the relative percentages of the Cu–W complex as a function of Cu(II) equivalents for the different DO3A–dendrons at generations 1 and 2.

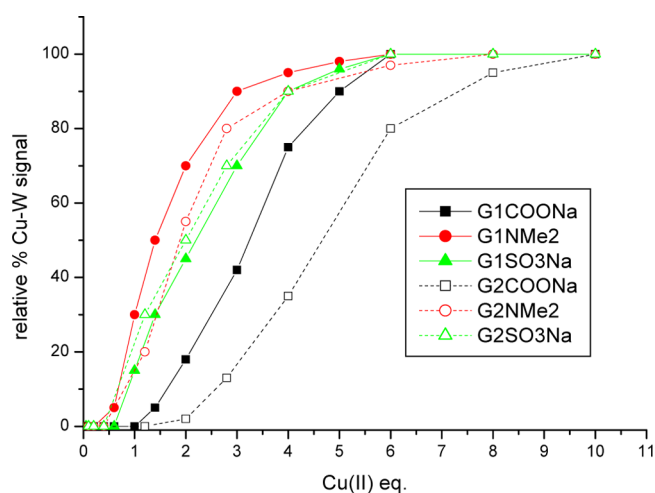


Figure 8. Relative percentages of the Cu–W complex as a function of Cu(II) equivalents for different DO3A–dendrons of generations 1 and 2.

This graph is profitably discussed together with the differences in the magnetic parameters of the Cu–N₄ coordination for the different dendrons (Table 3). These data indicate and summarize a number of trends discussed below.

For DO3AG_n(NMe₂)_m, the early saturation (at 0.5 equiv of Cu(II)) of G₁ (17) is still present for G₂ (18), but, in the latter case, the higher positive charge generates a moderate weakening of the Cu–N bonds (a small decrease in A_{zz} and increase in g_{zz} ,^{35–39} see Table 3). We found that a few more ions are allowed to interact with the DOTA core before saturation; this is because the weaker the bonds, the farther the ions are; therefore the Cu(II) ions at the DOTA core perturb each other to a lesser extent. In the cases of DO3AG_n(SO₃Na)_m, the higher negative charge of G₂ (12) compared to G₁ (11) favors a rather stronger Cu–N binding for G₂ (higher A_{zz} , lower g_{zz} ,^{35–39} and also lower mobility measured by τ ; see also Table 3) with respect to G₁ at the lowest Cu(II) concentrations. This suggests that the ions perturb each other when binding at the G₂ DO3A core, providing an earlier saturation of the DO3A nitrogen sites for G₂ compared to G₁ and different coordination modes for 11 and 12 (Table 3). However, by increasing the Cu(II) content, the discrepancy diminishes and the coordination behavior becomes similar for the two generations at the DO3A core.

For DO3AG_n(COONa)_m, the late appearance of Cu–W for 8 (at 2 Cu(II) equivalents, instead of 1 equivalent needed for 7) is nicely related to a clear involvement of the dendron branches (sulfur sites) in the complexation in solution. Indeed, a quite high amount (55%, see Table 3) of Cu–S₂O₂ is formed in solution for G₂ with 4 equiv of Cu(II). The Cu–S₂O₂ signal for 8 starts appearing at about 1.5 equiv of Cu(II) and progressively increases its relative percentage up to about 4 equiv. This means that a high amount of Cu(II) is needed for G₂ to saturate the dendron sulfur sites in solution. Conversely, for 7, the Cu–S₂O₂ signal starts contributing just above 0.2 equiv and reaches the maximum percentage at about 1.5 equiv. Therefore, each coordination shows a specific range of existence as a function of both the Cu(II) equivalents and the generation.

Here we have to underline that dendron 8 cannot be correctly analyzed by EPR above 4 equiv of Cu(II) due to precipitation of the complex. This means that precipitation occurs when Cu–S₂O₂ coordination is also saturated (after saturation of DO3A core complexation). We also found for G₂ dendrons a small but not negligible increase in the line widths of the EPR signals compared to G₁, due to weak spin–spin interactions arising from Cu(II) ions in quite close positions when saturation of the DO3A core complexation occurs. However, we may exclude that the ions lie in very close positions since the intensities of the Cu(II) spectra were almost the same in the absence and presence of the dendrons, and, therefore, strong spin–spin interactions do not occur in the examined Cu(II) concentration range.

All these results well describe the structural and dynamical properties of these dendrons and their Cu(II) complexes to be used for biomedical purposes. In this respect, the reproducibility over time (at least one month) of the EPR spectra characteristic of the Cu(II)–DO3A–dendron complexes in solution is again by itself a proof of the stability of these complexes, in agreement with the UV–vis data.

CONCLUSIONS

A synthetic protocol has been designed to incorporate the DO3A ligand to the focal point of cationic or anionic carbosilane dendrons. This procedure allows synthesizing and characterizing a set of bifunctional chelating agents (BFCAs) based on ionic carbosilane dendrons useful for several biomedical applications. The complexation behavior study of ionic BFCA seems to be an important parameter to be accomplished for considering potential applications. From the data obtained by UV–vis and EPR spectroscopy as well as potentiometric titrations, a number of trends can be summarized. The presence of the dendritic wedge as a substituent of the DOTA ligand originating DO3A ligands affords the strengthening of the chelate N₄ system with respect to the DOTA ligand, while the opposite is observed for the CYCLEN ligand. Therefore, the dendron branches may modify the complexation capacity of the macrocyclic ring compared to that of the DOTA ligand. Two different behaviors can be inferred depending on the nature of the ionic groups. For the carboxylate groups, important contributions of the dendritic branches to the coordination modes are detected through sulfur and carboxylate sites, Cu–S₂O₂. In this situation, the presence of such coordinating groups at the branches and periphery of the dendrons may be detrimental for some biomedical purposes such as diagnostic medicine. For instance, loading the dendrons with radioactive metal centers might result in some metal ions being weakly bound to the dendron. However, no contribution of branches through thioether groups in the coordinating mode was observed for sulfonate- or amine-terminated dendrons. Taking into account the weak coordination mode of the peripheral sulfonate or protonatable amine groups at the respective dendrons, radioactive metal centers can be easily located at the macrocycle fragment, leaving the dendritic surface for extra advantages, i.e., increasing solubility, interaction with nucleic acids in the case of amine-terminated dendrons, or antiviral properties for anionic sulfonate-terminated dendrons. Nevertheless, with regard to chelation chemistry, for example in neurodegenerative diseases, the three types of dendrons are ligands to be explored in the removal of critical metal ions such as Fe(III) and Cu(II). In this sense, the existence of new coordination modes in the carboxylate-terminated dendrons may be considered beneficial for this purpose.

The presence of higher generation dendrons on the DO3A ligand as substituents also produced different behaviors. While for the G₂ amine-terminated dendron the N₄ chelate interaction is destabilized with respect to G₁, the opposite is observed for the sulfonate-terminated dendrons. Concerning the carboxylate-terminated dendrons, their higher coordination capacity is also increased on increasing the generation, as result of a higher number of coordination sites at the branches, as expected. Surprisingly, for the second generation, Cu–S₂O₂ coordination is only observed from 1.5 equiv of Cu(II), probably due to the steric congestion of branches, which guide the metal interaction toward a preferred N₄ coordination mode. To sum up, our results show that G₂ carboxylate-terminated dendron followed distantly by the sulfonate-terminated dendrons present the optimal behavior, compared to the other dendrons, for complexing 1 equiv of Cu(II) at the DO3A core without competition with other interacting groups. For these compounds, stability studies in solution show that they are stable for at least 1 month, below 50° and at

physiological pH, which is fundamental for their biomedical use. All these tunable features are useful pieces of information from both chemical and biological points of view for the use of these dendrimers for biomedical purposes.

EXPERIMENTAL SECTION

Materials. All manipulations of oxygen- or water-sensitive compounds were carried out under an atmosphere of argon using standard Schlenk techniques. All solvents were dried and freshly distilled under argon prior to use, unless otherwise stated. Reagents were obtained from commercial sources and used as received.

Measurements. Spectroscopic analysis: ^1H , ^{13}C , ^{29}Si , and ^{15}N NMR spectra were recorded on Varian Unity VXR-300 and Varian 500 Plus instruments. Chemical shifts (δ , ppm) were measured relative to residual ^1H , ^{13}C , ^{29}Si , and ^{15}N resonances for CDCl_3 , D_2O , $\text{DMSO}-d_6$, and CD_3OD used as solvents. C, H analyses: They were carried out with a PerkinElmer 240 C microanalyzer. Mass spectra: Matrix-assisted laser desorption/ionization-time (MALDI-TOF) was obtained from a Bruker Ultraflex III. For MALDI-TOF samples 1,8,9-trihydroxyanthracene was used as the (dithranol) matrix. UV-vis analysis: A PerkinElmer Lambda 18 UV-vis spectrophotometer was used. Potentiometric titrations: These were performed using a CRISON titration system consisting of a digital potentiometer (BASIC 20+ pH-meter) and a pH electrode, which has an encapsulated reference system (cartridge) with a Ag^+ ion barrier, two diaphragms, and CRISOLYT electrolyte. The pH meter was standardized using an automatic recognition of technical buffers at pH's 4.01, 7.00, and 9.21 (25 °C). Samples were prepared by adding 20 mg of dendrons to 5 mL of H_2O (without ionic strength). First, the sample was basified with NaOH solution (0.01 M) to a pH = 12, and afterward, small quantities of a HCl solution (0.01 M) were added. In each addition the sample was stirred for 2 min, and then pH measurement was performed. EPR analysis: For the EPR analysis, the dendrons were dissolved in Millipore doubly distilled water, resulting in a final external surface group concentration of 0.1 M. Cupric nitrate hydrate ($\text{Cu}(\text{NO}_3)_2 \cdot 2.5\text{H}_2\text{O}$, Sigma-Aldrich, ACS reagent 98%) was also dissolved in Millipore doubly distilled water to obtain a final concentration, in the mixture with the dendrons, from 0.1 to 5 equiv. The samples were left equilibrating from 1 to 24 h (we verified that the spectra did not change in this time range). The EPR tubes have a constant internal diameter of 2 mm and were filled with 50 μL of solutions. EPR spectra were recorded by means of an EMX-Bruker spectrometer operating at X band (9.5 GHz) and interfaced with a PC (software from Bruker for handling the EPR spectra). The temperature was controlled with a Bruker ST3000 variable-temperature assembly cooled with liquid nitrogen. The EPR spectra were recorded for the different samples at 298 and 150 K. In all cases, we controlled the reproducibility of the results by repeating the EPR analysis (three times) in the same experimental conditions for each sample.

Synthesis of (CYCLEN) G_1V_2 (1). To a solution of CYCLEN (1.32 g, 7.72 mmol) in CHCl_3 (dry) was added slowly a solution of carbosilane dendron BrG_1V_2 (600 mg, 2.57 mmol) and NEt_3 (0.43 mL, 3.10 mmol). The reaction was stirred overnight at 60 °C. The solvent was removed under vacuum, the crude was dissolved in a mixture of $\text{Et}_2\text{O}/\text{H}_2\text{O}$ (1:1), the combined organic phase was dried with MgSO_4 , and the solvent was removed under vacuum. The residue was purified by size exclusion chromatography (a polystyrene stationary phase (Bio.Beads SX-1 by Bio-Rad)) in THF, which gave compound 1 as brown oil (0.550 g, 66% yield). ^1H NMR (CDCl_3): δ 0.10 (s, 3 H, SiMeC_2H_3), 0.62 (m, 2 H, $\text{CH}_2\text{SiC}_2\text{H}_3$), 1.33 (m, 2 H, $\text{CH}_2\text{CH}_2\text{Si}$), 1.50 (m, 2 H, NCH_2CH_2), 2.35–2.75 (m, 18 H, $\text{N}(\text{CH}_2)_2\text{N}$ and $\text{NCH}_2\text{CH}_2\text{CH}_2\text{CH}_2\text{Si}$), 5.70 (m, 2 H, SiCHCH_2), 6.16 (m, 4 H, SiCHCH_2). ^{13}C NMR (CDCl_3): δ –5.4 (MeSi), 13.9 (CH_2Si), 21.7 ($\text{NCH}_2\text{CH}_2\text{CH}_2\text{CH}_2\text{Si}$), 31.2 ($\text{NCH}_2\text{CH}_2\text{CH}_2\text{CH}_2\text{Si}$), 45.2–51.6 ($\text{N}(\text{CH}_2)_2\text{N}$), 54.1 ($\text{NCH}_2\text{CH}_2\text{CH}_2\text{CH}_2\text{Si}$), 132.7 (SiCHCH_2), 137.1 (SiCHCH_2). ^{15}N NMR (CDCl_3): δ 20.5 (NH), 28.7 (NCH_2). ^{29}Si NMR (CDCl_3): δ –12.9 (SiMeC_2H_3). HPLC-MS (crude product): 78% mono:22% disubstitution. MS: $[\text{M} + \text{H}]^+ = 325.23$ uma (calcd = 325.58 uma).

Synthesis of (CYCLEN) G_2V_4 (2). The reaction of CYCLEN (376 mg, 2.18 mmol) with carbosilane dendron BrG_2V_4 (500 mg, 1.09 mmol) and NEt_3 (0.18 mL, 1.29 mmol) was carried out in the similar way to the synthesis of 1. Compound 2 was obtained as a brown oil (450 mg, 75% yield). ^1H NMR (CDCl_3): δ –0.13 (s, 3 H, SiMe), 0.09 (s, 6 H, SiMeC_2H_3), 0.46–0.56 (m, 6 H, SiCH_2), 0.66 (m, 4 H, $\text{CH}_2\text{SiC}_2\text{H}_3$), 1.21–1.42 (m, 8 H, $\text{CH}_2\text{CH}_2\text{Si}$ and NCH_2CH_2), 2.36–2.76 (m, 18 H, $\text{N}(\text{CH}_2)_2\text{N}$ and $\text{NCH}_2\text{CH}_2\text{CH}_2\text{CH}_2\text{Si}$), 5.65 (m, 4 H, SiCHCH_2), 6.06 (m, 8 H, SiCHCH_2). $^{13}\text{C}\{^1\text{H}\}$ NMR (CDCl_3): δ –5.1 and 5.2 (MeSi), 13.9 (SiCH_2), 18.2 and 18.7 (CH_2), 21.7 ($\text{NCH}_2\text{CH}_2\text{CH}_2\text{CH}_2\text{Si}$), 31.2 ($\text{NCH}_2\text{CH}_2\text{CH}_2\text{CH}_2\text{Si}$), 45.15–51.19 ($\text{N}(\text{CH}_2)_2\text{N}$), 54.3 ($\text{NCH}_2\text{CH}_2\text{CH}_2\text{CH}_2\text{Si}$), 132.6 (SiCHCH_2), 137.0 (SiCHCH_2). ^{15}N NMR (CDCl_3): δ 20.5 (NH), 28.7 (NCH_2). ^{29}Si NMR (CDCl_3): δ 1.7 (SiMe)–13.5 (SiCHCH_2). HPLC-MS (crude product): 85% mono:15% disubstitution. MS: $[\text{M} + \text{H}]^+ = 549.42$ uma (calcd = 549.41 uma).

Synthesis of [DO3A(O t Bu) $_3$] G_1V_2 (3). A solution of compound 1 (0.500 g, 1.54 mmol), *tert*-butyl bromoacetate (0.73 mL, 4.95 mmol), and K_2CO_3 (1.28 g, 9.22 mmol) in 10 mL of acetonitrile was heated at 60 °C for 24 h. The solvent was removed under vacuum, the crude was dissolved in a mixture of $\text{Et}_2\text{O}/\text{H}_2\text{O}$ (1:1), the combined organic phase was dried with MgSO_4 , and the solvent was removed under vacuum. The residue was purified by size exclusion chromatography (a polystyrene stationary phase (Bio.Beads SX-1 by Bio-Rad)) in THF, which gave compound 3 as a brown oil (0.710 g, 69% yield). ^1H NMR (CDCl_3): δ 0.10 (s, 3 H, SiMeC_2H_3), 0.63 (m, 2 H, $\text{CH}_2\text{SiC}_2\text{H}_3$), 1.32 (m, 2 H, $\text{CH}_2\text{CH}_2\text{Si}$), 1.38 (s, 18 H, $\text{C}(\text{CH}_3)_3$), 1.44 (s, 9 H, $\text{C}(\text{CH}_3)_3$), 1.67 (m, 2 H, NCH_2CH_2), 2.6–3.73 (m, 22 H, $\text{N}(\text{CH}_2)_2\text{N}$ and NCH_2COO), 3.68 (m, 2 H, NCH_2CH_2), 5.70 (m, 2 H, SiCHCH_2), 6.16 (m, 4 H, SiCHCH_2). $^{13}\text{C}\{^1\text{H}\}$ NMR (CDCl_3): δ –5.5 (MeSi), 13.9 (SiCH_2), 21.0 ($\text{NCH}_2\text{CH}_2\text{CH}_2\text{CH}_2\text{Si}$), 28.2 ($\text{C}(\text{CH}_3)_3$), 31.2 ($\text{NCH}_2\text{CH}_2\text{CH}_2\text{CH}_2\text{Si}$), 47.5–60.3 ($\text{N}(\text{CH}_2)_2\text{N}$ and $\text{NCH}_2\text{CH}_2\text{CH}_2\text{CH}_2\text{Si}$), 81.7 ($\text{C}(\text{CH}_3)_3$), 133.3 (SiCHCH_2), 136.2 (SiCHCH_2), 170.15, 170.6 (COO). ^{29}Si NMR (CDCl_3): δ –13.0 (SiMeC_2H_3). Anal. Calcd for $\text{C}_{35}\text{H}_{66}\text{N}_4\text{O}_6\text{Si}$ (667.01 g/mol) (KBr): C, 53.48; H, 8.46; N, 7.13. Found: C, 54.96; H, 9.34; N, 7.13. MS: $[\text{M} + \text{H}]^+ = 667.48$ uma (calcd = 667.48 uma).

Synthesis of [DO3A(O t Bu) $_3$] G_2V_4 (4). The reaction of compound 2 (300 mg, 0.546 mmol) with *tert*-butyl bromoacetate (0.28 mL, 1.89 mmol) and K_2CO_3 (0.377 g, 2.72 mmol) was carried out in the similar way to the synthesis of 3. Compound 4 was obtained as a brown oil (370 mg, 75% yield). ^1H NMR (CDCl_3): δ –0.13 (s, 3 H, SiMe), 0.09 (s, 6 H, SiMeC_2H_3), 0.50 (m, 6 H, SiCH_2), 0.67 (m, 4 H, $\text{CH}_2\text{SiC}_2\text{H}_3$), 1.29 (m, 8 H, $\text{CH}_2\text{CH}_2\text{Si}$ and NCH_2CH_2), 1.42 (s, 18 H, $\text{C}(\text{CH}_3)_3$), 1.47 (s, 9 H, $\text{C}(\text{CH}_3)_3$), 2.6–3.7 (m, 22 H, $\text{N}(\text{CH}_2)_2\text{N}$ and NCH_2COO), 3.68 (m, 2 H, NCH_2CH_2), 5.65 (m, 4 H, SiCHCH_2), 6.05 (m, 8 H, SiCHCH_2). ^{13}C NMR (CDCl_3): δ –5.3 (MeSi), 14.0 (SiCH_2), 18.3 (CH_2), 21.0 ($\text{NCH}_2\text{CH}_2\text{CH}_2\text{CH}_2\text{Si}$), 22.3 (CH_2), 28.3 ($\text{C}(\text{CH}_3)_3$), 33.2 ($\text{NCH}_2\text{CH}_2\text{CH}_2\text{CH}_2\text{Si}$), 48.7–59.0 ($\text{N}(\text{CH}_2)_2\text{N}$ and $\text{NCH}_2\text{CH}_2\text{CH}_2\text{CH}_2\text{Si}$), 81.7 ($\text{C}(\text{CH}_3)_3$), 132.8 (SiCHCH_2), 136.7 (SiCHCH_2), 170.4, 170.6 (COO). ^{29}Si NMR (CDCl_3): δ 1.8 (SiMe), –13.5 (SiCHCH_2). Anal. Calcd for $\text{C}_{47}\text{H}_{90}\text{N}_4\text{O}_6\text{Si}_3$ (891.50 g/mol) (KBr): C, 55.86; H, 8.98; N, 5.54. Found: C, 55.32; H, 9.16; N, 4.99. MS: $[\text{M} + \text{Na}]^+ = 913.62$ uma (calcd = 913.62 uma).

Synthesis of [DO3A(O t Bu) $_3$] G_1 (COOMe) $_2$ (5). Methyl sulfanylacetate (0.11 mL, 1.21 mmol) and 10% molar DMPA (0.032 g, 0.125 mmol) was added to a 1:1 THF/MeOH (4 mL) solution of compound 3 (0.400 g, 0.600 mmol). The reaction mixture was deoxygenated and irradiated with a UV lamp for 4 h. The initial reaction mixture was concentrated via rotary evaporation, and the residue was purified by size exclusion chromatography (a polystyrene stationary phase (Bio.Beads SX-1 by Bio-Rad)) in THF, which gave compound 5 as a yellow oil (0.420 g, 80% yield). ^1H NMR (CDCl_3): δ 0.01 (s, 3 H, SiMe), 0.59 (m, 2 H, CH_2Si), 0.88 (t, 4 H, $\text{SiCH}_2\text{CH}_2\text{S}$), 1.29 (m, 2 H, $\text{CH}_2\text{CH}_2\text{Si}$), 1.43 (s, 18 H, $\text{C}(\text{CH}_3)_3$), 1.45 (m, 11 H, $\text{C}(\text{CH}_3)_3$ and NCH_2CH_2), 1.90–3.70 (m, 24 H, $\text{N}(\text{CH}_2)_2\text{N}$, NCH_2COO , and NCH_2CH_2), 2.63 (t, 4 H, $\text{SiCH}_2\text{CH}_2\text{S}$), 3.22 (s, 4 H, SCH_2COOMe), 3.71 (s, 6 H, SCH_2COOMe). $^{13}\text{C}\{^1\text{H}\}$ NMR (CDCl_3): δ –5.4 (MeSi), 13.6 (SiCH_2 and $\text{SiCH}_2\text{CH}_2\text{S}$), 20.8 ($\text{NCH}_2\text{CH}_2\text{CH}_2\text{CH}_2\text{Si}$), 28.1 ($\text{C}(\text{CH}_3)_3$ and $\text{SiCH}_2\text{CH}_2\text{S}$), 33.2

(NCH₂CH₂CH₂CH₂Si and SCH₂COOMe), 47.5–60.3 (N(CH₂)₂N and NCH₂CH₂CH₂CH₂Si), 52.4 (SCH₂COOMe), 81.6 (C(CH₃)₃), 170.15, 170.6, 170.9 (COOMe and COO). ²⁹Si NMR (CDCl₃): δ 3.1 (SiCH₂CH₂S). Anal. Calcd for C₄₁H₇₈N₄O₁₀S₂Si (878.29 g/mol) (KBr): C, 49.33; H, 7.88; N, 5.61; S, 6.42. Found: C, 50.20; H, 7.27; N, 4.48; S, 6.58. MS: [M + H]⁺ = 879.50 uma (calcd = 879.49 uma).

Synthesis of [DO3A(OⁱBu)₃]G₂(COOMe)₄ (6). The reaction of compound 4 (0.450 g, 0.505 mmol), methyl sulfanylacetate (0.21 mL, 2.31 mmol), and DMPA (0.058 g, 0.226 mmol) was carried out in a similar way to that for the synthesis of compound 5. Compound 6 was obtained as a yellow oil (0.500 g, 75% yield). ¹H NMR (CDCl₃): δ –0.10 (s, 3 H, SiMe), 0.01 (s, 6 H, SiMe), 0.55 (m, 10 H, SiCH₂), 0.88 (t, 8 H, SiCH₂CH₂S), 1.28 (m, 8 H, CH₂CH₂Si and NCH₂CH₂), 1.42 (s, 27 H, C(CH₃)₃), 1.90–3.70 (m, 24 H, N(CH₂)₂N, NCH₂COO, and NCH₂CH₂), 2.63 (m, 8 H, SiCH₂CH₂S), 3.22 (s, 8 H, SCH₂COOMe), 3.70 (s, 12 H, SCH₂COOMe). ¹³C{¹H} NMR (CDCl₃): δ –5.4 (MeSi), 13.9 (SiCH₂ and SiCH₂CH₂S), 18.2 (NCH₂CH₂CH₂CH₂Si), 28.2 (C(CH₃)₃ and SiCH₂CH₂S), 33.3 (NCH₂CH₂CH₂CH₂Si and SCH₂COOMe), 58.7 (SCH₂COOMe), 81.9 (C(CH₃)₃), 170.9 (COOMe). ²⁹Si NMR (CDCl₃): δ 1.65 (SiMe), 2.37 (SiCH₂CH₂S). Anal. Calcd for C₅₉H₁₁₄N₄O₁₄S₄Si₃·KBr (1314.65 g/mol): C, 49.38; H, 8.01; N, 3.90; S, 8.94. Found: C, 48.72; H, 7.64; N, 3.94; S, 8.54. MS: [M + H]⁺ = 1315.66 uma (calcd = 1315.65 uma).

Synthesis of DO3AG₁(COONa)₂ (7). In a methanol (5 mL) solution of compound 5 (0.150 g, 0.171 mmol), a NaOH solution was added drop by drop (0.068 g, 1.71 mmol), and the reaction mixture was stirred overnight. The reaction mixture was concentrated, washed with ether, and then dissolved in water. The residue was purified by size exclusion chromatography in water (Sephadex), which gave compound 7 as a yellow solid (0.075 g, 56% yield). ¹H NMR (D₂O): δ –0.09 (s, 3 H, SiMe), 0.51 (m, 2 H, CH₂Si), 0.81 (t, 4 H, SiCH₂CH₂S), 1.28 (m, 4 H, CH₂CH₂Si and NCH₂CH₂), 1.90–3.80 (m, 24 H, N(CH₂)₂N, NCH₂COO, NCH₂CH₂), 2.51 (t, 4 H, SiCH₂CH₂S), 3.06 (s, 4 H, SCH₂COONa). ¹³C{¹H} NMR (D₂O): δ –5.2 (MeSi), 13.5 (SiCH₂), 14.4 (SiCH₂CH₂S), 21.1 (NCH₂CH₂CH₂CH₂Si), 29.6 (NCH₂CH₂CH₂CH₂Si), 28.3 (SiCH₂CH₂S), 37.9 (SCH₂COONa), 47.6–57.2 (N(CH₂)₂N and NCH₂CH₂CH₂CH₂Si), 179.4 and 179.8 (COONa). ²⁹Si NMR (D₂O): δ 2.65 (SiCH₂CH₂S). Anal. Calcd for C₂₇H₄₅N₄Na₅O₁₀S₂Si (792.83 g/mol): C, 40.90; H, 5.72; N, 7.07; S, 8.09. Found: C, 40.27; H, 5.08; N, 6.98; S, 8.05.

Synthesis of DO3AG₂(COONa)₄ (8). The reaction of compound 6 (0.300 g, 0.228 mmol) with NaOH (0.127 g, 3.17 mmol) was carried out in a similar way to that for the synthesis of compound 7. This dendron was purified by nanofiltration using a M_w = 500 membrane. The pure product was dried *in vacuo* to afford compound 8 as a yellow solid (0.215 g, 76% yield). ¹H NMR (D₂O): δ –0.14 (s, 3 H, SiMe), –0.06 (s, 6 H, SiMe), 0.55 (m, 10 H, SiCH₂), 0.84 (t, 8 H, SiCH₂CH₂S), 1.28 (m, 8 H, CH₂CH₂Si and NCH₂CH₂), 1.90–3.70 (m, 24 H, N(CH₂)₂N, NCH₂COO, and NCH₂CH₂), 2.53 (m, 8 H, SiCH₂CH₂S), 3.12 (s, 8 H, SCH₂COONa). ¹³C{¹H} NMR (D₂O): –5.4 and 5.1 (MeSi), 14.4 (SiCH₂CH₂S), 12.2–20.4 (SiCH₂CH₂CH₂Si), 21.1 (NCH₂CH₂CH₂CH₂Si), 28.4 (SiCH₂CH₂S), 37.2 (NCH₂CH₂CH₂CH₂Si), 45.1–63.1 (N(CH₂)₂N and NCH₂CH₂CH₂CH₂Si), 178.8 (COONa). ²⁹Si NMR (D₂O): δ 1.59 (SiMe), 2.13 (SiCH₂CH₂S). Anal. Calcd for C₄₃H₇₅N₄Na₇O₁₄S₄Si₃·NaBr (1245.52 g/mol): C, 40.71; H, 5.96; N, 4.42; S, 10.11. Found: C, 40.41; H, 6.02; N, 3.59; S, 11.71.

Synthesis of [DO3A(OⁱBu)₃]G₁(SO₃Na)₂ (9). To a 1:2:1 THF/MeOH/H₂O solution (5 mL) of compound 3 (0.400 g, 0.600 mmol) were added in twice sodium 3-mercaptopropyl-1-propanesulfonate (0.224 g, 1.26 mmol) and 10% molar DMPA (0.032 g, 0.125 mmol). The reaction mixture was deoxygenated and irradiated with a UV lamp for 4 h. The initial reaction mixture was concentrated via rotary evaporation and solved in water. Attempts to purify this compound for analysis by using different methods failed because of its lack of solubility in water and most organic solvents (only soluble in DMSO). Nevertheless purification was achieved in the subsequent reaction to prepare 11 due to its solubility in water. ¹H NMR (DMSO-*d*₆): δ 0.00 (s, 3 H, SiMe), 0.60 (m, 2 H, CH₂Si), 0.83 (t, 4 H, SiCH₂CH₂S), 1.29

(m, 2 H, CH₂CH₂Si), 1.41 (s, 29 H, C(CH₃)₃ and NCH₂CH₂), 1.90–3.70 (m, 24 H, N(CH₂)₂N, NCH₂COO, and NCH₂CH₂), 1.81 (m, 4 H, SCH₂CH₂CH₂SO₃Na), 2.54 (m, 8 H, SCH₂CH₂CH₂SO₃Na and SiCH₂CH₂S), 3.15 (t, 4 H, SCH₂CH₂CH₂SO₃Na, overlapped with residual water).

Synthesis of [DO3A(OⁱBu)₃]G₂(SO₃Na)₄ (10). The reaction of compound 4 (0.450 g, 0.505 mmol) with sodium 3-mercaptopropyl-1-propanesulfonate (0.404 g, 2.27 mmol) and 10% molar DMPA (0.058 g, 0.226 mmol) was carried out in a similar way to that for the synthesis of compound 9. This dendron was purified by nanofiltration using a M_w = 500 membrane. The pure product was dried *in vacuo* to afford compound 10 as a yellow solid (0.650 g, 80% yield). ¹H NMR (D₂O): δ –0.13 (s, 3 H, SiMe), 0.01 (s, 6 H, SiMe), 0.53 (m, 10 H, CH₂Si), 0.87 (t, 8 H, SiCH₂CH₂S), 1.39 (m, 35 H, CH₂CH₂Si, NCH₂CH₂, and C(CH₃)₃), 1.90–3.70 (m, 24 H, N(CH₂)₂N, NCH₂COO, and NCH₂CH₂), 1.93 (m, 8 H, SCH₂CH₂CH₂SO₃Na), 2.58 (m, 16 H, SCH₂CH₂CH₂SO₃Na and SiCH₂CH₂S), 2.84 (s, 8 H, SCH₂CH₂CH₂SO₃Na). ¹³C{¹H} NMR (D₂O): δ –5.1 (MeSi), 13.1 (SiCH₂), 14.3 (SiCH₂CH₂S), 18.4 (NCH₂CH₂CH₂CH₂Si), 27.9 (C(CH₃)₃), 24.4 (SCH₂CH₂CH₂SO₃Na), 26.8 (SiCH₂CH₂S), 30.2 (SCH₂CH₂CH₂SO₃Na), 36.8 (NCH₂CH₂CH₂CH₂Si), 50.1 (SCH₂CH₂CH₂SO₃Na), 56.4 (NCH₂CH₂CH₂CH₂Si), 81.6 (C(CH₃)₃), 165.4 (COO). ²⁹Si NMR (D₂O): δ 1.71 (SiMe), 2.13 (SiCH₂CH₂S). Anal. Calcd for C₅₉H₁₁₈N₄Na₄O₁₈S₈Si₃·KBr (1604.32 g/mol): C, 41.52; H, 6.90; N, 3.25; S, 14.89. Found: C, 41.59; H, 7.56; N, 2.95; S, 16.93.

Synthesis of DO3AG₁(SO₃Na)₂ (11). To a MeOH/H₂O (2:1) solution of compound 9 (0.150 g, 0.147 mmol) was added drop by drop a NaOH solution (0.053 g, 1.32 mmol), and the reaction mixture was stirred for 2 h. The reaction mixture was concentrated, washed with ether, and then dissolved in water. The residue was purified by size exclusion chromatography in water (Sephadex), which gave compound 11 as a yellow solid (0.090 g, 67% yield). ¹H NMR (D₂O): δ –0.06 (s, 3 H, SiMe), 0.55 (m, 2 H, CH₂Si), 0.85 (t, 4 H, SiCH₂CH₂S), 1.39 (m, 4 H, CH₂ and CH₂SiNCH₂CH₂), 1.90–3.70 (m, 24 H, N(CH₂)₂N, NCH₂COO, and NCH₂CH₂), 1.90 (m, 4 H, SCH₂CH₂CH₂SO₃Na), 2.57 (m, 8 H, SCH₂CH₂CH₂SO₃Na and SiCH₂CH₂S), 2.89 (s, 4 H, SCH₂CH₂CH₂SO₃Na). ¹³C{¹H} NMR (D₂O): δ –5.2 (MeSi), 13.7 (SiCH₂), 14.5 (SiCH₂CH₂S), 21.1 (NCH₂CH₂CH₂CH₂Si), 25.3 (SCH₂CH₂CH₂SO₃Na), 27.6 (SiCH₂CH₂S), 29.6 (SCH₂CH₂CH₂SO₃Na), 45.15–56.4 (N(CH₂)₂N and NCH₂CH₂CH₂CH₂Si), 51.1 (SCH₂CH₂CH₂SO₃Na), 170.5, 171.93 (COO). ²⁹Si NMR (D₂O): δ 3.1 (SiCH₂CH₂S). Anal. Calcd for C₂₉H₅₃N₄Na₅O₁₂S₄Si (921.05 g/mol): C, 37.82; H, 5.80; N, 6.08; S, 13.93. Found: C, 36.79; H, 6.21; N, 4.89; S, 11.02.

Synthesis of DO3AG₂(SO₃Na)₄ (12). The reaction of compound 10 (0.300 g, 0.187 mmol) with NaOH (0.045 g, 1.12 mmol) was carried out in a similar way to that for the synthesis of compound 11. This dendron was purified by nanofiltration using a M_w = 500 membrane. The pure product was dried *in vacuo* to afford compound 12 as a yellow solid (0.215 g, 77% yield). ¹H NMR (D₂O): δ –0.10 (s, 3 H, SiMe), –0.01 (s, 6 H, SiMe), 0.55 (m, 10 H, CH₂Si), 0.85 (t, 8 H, SiCH₂CH₂S), 1.31 (m, 8 H, CH₂CH₂Si and NCH₂CH₂), 1.90–3.70 (m, 24 H, N(CH₂)₂N, NCH₂COO, and NCH₂CH₂), 1.92 (m, 8 H, SCH₂CH₂CH₂SO₃Na), 2.59 (m, 16 H, SCH₂CH₂CH₂SO₃Na and SiCH₂CH₂S), 2.87 (s, 8 H, SCH₂CH₂CH₂SO₃Na). ¹³C{¹H} NMR (D₂O): δ –5.2 (MeSi), 13.5 (SiCH₂), 14.3 (SiCH₂CH₂S), 21.5 (NCH₂CH₂CH₂CH₂Si), 24.3 (SCH₂CH₂CH₂SO₃Na), 27.0 (SiCH₂CH₂S), 30.1 (SCH₂CH₂CH₂SO₃Na), 50.1 (SCH₂CH₂CH₂SO₃Na), 190.4 (COO). ²⁹Si NMR (D₂O): δ 1.20 (SiMe), 2.12 (SiCH₂CH₂S). Anal. Calcd for C₄₇H₉₁N₄Na₇O₁₈S₈Si₃ (1501.95 g/mol): C, 37.58; H, 6.11; N, 3.73; S, 17.08. Found: C, 37.27; H, 5.08; N, 2.24.

Synthesis of [DO3A(OⁱBu)₃]G₁(NMe₂·HCl)₂ (13). 2-(Dimethylamino)ethanethiol hydrochloride (0.223 g, 1.57 mmol) and 5% molar DMPA (0.021 g, 0.08 mmol) were added to a 1:2 THF/methanol solution (4 mL) of compound 3 (0.500 g, 0.750 mmol). The reaction mixture was deoxygenated and irradiated with a UV lamp for 2 h. Another 5% molar DMPA was added, and the reaction mixture was irradiated for another 2 h. The initial reaction mixture was

concentrated via rotary evaporation and dissolved in water. This polymer was purified by nanofiltration in which a $M_w = 500$ membrane was used. The pure product was dried under vacuum to afford compound **13** as a hygroscopic yellow solid (0.370 g, 52% yield). ^1H NMR (DMSO- d_6): δ 0.03 (s, 3 H, SiMe), 0.59 (m, 2 H, CH_2Si), 0.87 (t, 4 H, $\text{SiCH}_2\text{CH}_2\text{S}$), 1.28 (m, 2 H, $\text{CH}_2\text{CH}_2\text{Si}$), 1.41 (s, 18 H, $\text{C}(\text{CH}_3)_3$), 1.46 (s, 9 H, $\text{C}(\text{CH}_3)_3$ and m, 2 H, NCH_2CH_2), 1.90–3.80 (24 H, m, NCH_2COO , NCH_2CH_2 , $\text{N}(\text{CH}_2)_2\text{N}$), 2.53 (4 H, $\text{SiCH}_2\text{CH}_2\text{S}$), 2.71 (12 H, $\text{SCH}_2\text{CH}_2\text{NMe}_2\text{HCl}$), 2.88 (t, 4 H, $\text{SCH}_2\text{CH}_2\text{NMe}_2\text{HCl}$), 3.17 (m, 4 H, $\text{SCH}_2\text{CH}_2\text{NMe}_2\text{HCl}$). $^{13}\text{C}\{^1\text{H}\}$ NMR (DMSO- d_6): δ –5.2 (MeSi), 13.1 (SiCH_2), 14.4 ($\text{SiCH}_2\text{CH}_2\text{S}$), 21.1 ($\text{NCH}_2\text{CH}_2\text{CH}_2\text{CH}_2\text{Si}$), 26.9 ($\text{SiCH}_2\text{CH}_2\text{S}$), 28.2 ($\text{C}(\text{CH}_3)_3$), 31.2 ($\text{NCH}_2\text{CH}_2\text{CH}_2\text{CH}_2\text{Si}$), 45.15–51.19 ($\text{N}(\text{CH}_2)_2\text{N}$), 42.4 ($\text{SCH}_2\text{CH}_2\text{NMe}_2\text{HCl}$), 42.5 ($\text{SCH}_2\text{CH}_2\text{NMe}_2\text{HCl}$), 56.4 ($\text{SCH}_2\text{CH}_2\text{NMe}_2\text{HCl}$), 67.4 ($\text{NCH}_2\text{CH}_2\text{CH}_2\text{CH}_2\text{Si}$), 81.1 ($\text{C}(\text{CH}_3)_3$), 170.7 (CO). ^{29}Si NMR (DMSO- d_6): δ 3.1 ($\text{SiCH}_2\text{CH}_2\text{S}$). Attempts to obtain accurate analytical data failed because of its high hygroscopic behavior. Nevertheless good analytical data were achieved in the subsequent reaction to prepare **15** where water is avoided in the purification process.

Synthesis of $[\text{DO3A}(\text{O}^t\text{Bu})_3]\text{G}_2(\text{NMe}_2)_4$ (14**).** The reaction of compound **4** (0.270 g, 0.302 mmol), 2-(dimethylamino)ethanethiol hydrochloride (0.193 g, 1.36 mmol), and 5% molar DMPA (0.018 g, 0.070 mmol) was carried out in a similar way to that for the synthesis of **13**. Compound **14** was obtained as a hygroscopic yellow solid (0.323 g, 75% yield). ^1H NMR (DMSO- d_6): δ –0.08 (s, 3 H, SiMe), 0.02 (s, 6 H, SiMe), 0.54 (m, 10 H, SiCH_2), 0.85 (t, 8 H, $\text{SiCH}_2\text{CH}_2\text{S}$), 1.27 (m, 8 H, $\text{CH}_2\text{CH}_2\text{Si}$ and NCH_2CH_2), 1.41 (27 H, m, $\text{C}(\text{CH}_3)_3$), 1.90–3.70 (m, 24 H, $\text{N}(\text{CH}_2)_2\text{N}$, NCH_2COO , and NCH_2CH_2), 2.60 (t, 8 H, $\text{SiCH}_2\text{CH}_2\text{S}$), 2.74 (s, 24 H, $\text{SCH}_2\text{CH}_2\text{NMe}_2\text{HCl}$), 2.86 (t, 8 H, $\text{SCH}_2\text{CH}_2\text{NMe}_2\text{HCl}$), 3.21 (m, 8 H, $\text{SCH}_2\text{CH}_2\text{NMe}_2\text{HCl}$). $^{13}\text{C}\{^1\text{H}\}$ NMR (DMSO- d_6): δ –5.1 and 4.7 (MeSi), 13.1 (SiCH_2), 14.4 ($\text{SiCH}_2\text{CH}_2\text{S}$), 25.2 ($\text{NCH}_2\text{CH}_2\text{CH}_2\text{CH}_2\text{Si}$), 26.9 ($\text{SiCH}_2\text{CH}_2\text{S}$), 28.3 ($\text{C}(\text{CH}_3)_3$), 31.2 ($\text{NCH}_2\text{CH}_2\text{CH}_2\text{CH}_2\text{Si}$), 45.15–51.19 ($\text{N}(\text{CH}_2)_2\text{N}$), 42.3 ($\text{SCH}_2\text{CH}_2\text{NMe}_2\text{HCl}$ and $\text{SCH}_2\text{CH}_2\text{NMe}_2\text{HCl}$), 56.2 ($\text{SCH}_2\text{CH}_2\text{NMe}_2\text{HCl}$), 67.4 ($\text{NCH}_2\text{CH}_2\text{CH}_2\text{CH}_2\text{Si}$), 81.4 ($\text{C}(\text{CH}_3)_3$), 170.7 (CO). ^{29}Si NMR (DMSO- d_6): δ 1.9 (SiMe), 2.6 ($\text{SiCH}_2\text{CH}_2\text{S}$). Attempts to obtain accurate analytical data failed because of its high hygroscopic behavior. Nevertheless good analytical data were achieved in the subsequent reaction to prepare **16**, where water is avoided in the purification process.

Synthesis of $[\text{DO3A}(\text{O}^t\text{Bu})_3]\text{G}_1(\text{NMe}_2)_2$ (15**).** In a $\text{H}_2\text{O}/\text{CH}_2\text{Cl}_2$ (1:1, 20 mL) solution of compound **13** (0.300 g, 0.316 mmol), 1 mL of a saturated aqueous solution of Na_2CO_3 was added dropwise. The reaction mixture was stirred for 10 min at room temperature, and finally the aqueous phase was removed. The organic phase was dried under vacuum to get compound **15** as pale yellow oil (0.255 g, 92% yield). ^1H NMR (CDCl_3): δ 0.04 (s, 3 H, SiMe), 0.55 (m, 2 H, CH_2Si), 0.87 (t, 4 H, $\text{SiCH}_2\text{CH}_2\text{S}$), 1.29 (m, 2 H, $\text{CH}_2\text{CH}_2\text{Si}$), 1.42 (s, 18 H, $\text{C}(\text{CH}_3)_3$), 1.48 (m, 11 H, $\text{C}(\text{CH}_3)_3$ and NCH_2CH_2), 1.90–3.70 (m, 24 H, $\text{N}(\text{CH}_2)_2\text{N}$, NCH_2COO , and NCH_2CH_2), 2.23 (s, 12 H, $\text{SCH}_2\text{CH}_2\text{NMe}_2$), 2.45 (m, 4 H, $\text{SCH}_2\text{CH}_2\text{NMe}_2$), 2.48 (t, 4 H, $\text{SiCH}_2\text{CH}_2\text{S}$), 2.59 (t, 4 H, $\text{SCH}_2\text{CH}_2\text{NMe}_2$). $^{13}\text{C}\{^1\text{H}\}$ NMR (CDCl_3): δ –5.2 (MeSi), 13.1 (SiCH_2), 14.4 ($\text{SiCH}_2\text{CH}_2\text{S}$), 20.9 ($\text{NCH}_2\text{CH}_2\text{CH}_2\text{CH}_2\text{Si}$), 28.7 ($\text{C}(\text{CH}_3)_3$), 29.6 ($\text{SiCH}_2\text{CH}_2\text{S}$), 36.3 ($\text{NCH}_2\text{CH}_2\text{CH}_2\text{CH}_2\text{Si}$), 45.15–51.19 ($\text{N}(\text{CH}_2)_2\text{N}$), 45.0 ($\text{SCH}_2\text{CH}_2\text{NMe}_2$), 52.6 ($\text{SCH}_2\text{CH}_2\text{NMe}_2$), 58.9 ($\text{SCH}_2\text{CH}_2\text{NMe}_2$), 81.4 ($\text{C}(\text{CH}_3)_3$), 170.6 (CO). ^{29}Si NMR (CDCl_3): δ 2.8 ($\text{SiCH}_2\text{CH}_2\text{S}$). Anal. Calcd for $\text{C}_{43}\text{H}_{88}\text{N}_6\text{O}_6\text{S}_2\text{Si}_3\text{NaCl}$ (877.41 g/mol): C, 55.19; H, 9.48; N, 8.98; S, 6.85. Found: C, 56.11.43; H, 8.45; N, 8.08; S, 6.89. MS: $[\text{M} + \text{H}]^+ = 877.40$ uma (calcd = 877.60 uma).

Synthesis of $[\text{DO3A}(\text{O}^t\text{Bu})_3]\text{G}_2(\text{NMe}_2)_4$ (16**).** The reaction of compound **14** (0.250 g, 0.171 mmol) with Na_2CO_3 (1 mL) was carried out in a similar way to that for the synthesis of **15**. Compound **16** was obtained as a pale yellow oil (0.210 g, 93% yield). ^1H NMR (CDCl_3): δ –0.11 (s, 3 H, SiMe), 0.05 (s, 6 H, SiMe), 0.55 (m, 10 H, SiCH_2), 0.87 (t, 8 H, $\text{SiCH}_2\text{CH}_2\text{S}$), 1.21–1.42 (m, 8 H, $\text{CH}_2\text{CH}_2\text{Si}$ and NCH_2CH_2), 1.42 (s, 27 H, $\text{C}(\text{CH}_3)_3$), 1.90–3.70 (m, 24 H, $\text{N}(\text{CH}_2)_2\text{N}$, NCH_2COO , and NCH_2CH_2), 2.25 (s, 24 H, $\text{SCH}_2\text{CH}_2\text{NMe}_2$), 2.48–2.62 (m, 8 H, $\text{SCH}_2\text{CH}_2\text{NMe}_2$, 8 H,

$\text{SiCH}_2\text{CH}_2\text{S}$, 8 H, $\text{SCH}_2\text{CH}_2\text{NMe}_2$). $^{13}\text{C}\{^1\text{H}\}$ NMR (CDCl_3): δ –5.1 and 5.2 (MeSi), 13.9 (SiCH_2), 14.7 ($\text{SiCH}_2\text{CH}_2\text{S}$), 18.4 (CH_2), 22.5 ($\text{NCH}_2\text{CH}_2\text{CH}_2\text{CH}_2\text{Si}$), 27.7 ($\text{C}(\text{CH}_3)_3$), 29.6 ($\text{SiCH}_2\text{CH}_2\text{S}$), 36.8 ($\text{NCH}_2\text{CH}_2\text{CH}_2\text{CH}_2\text{Si}$), 45.4 ($\text{SCH}_2\text{CH}_2\text{NMe}_2$), 52.6 ($\text{SCH}_2\text{CH}_2\text{NMe}_2$), 56.2 ($\text{SCH}_2\text{CH}_2\text{NMe}_2$), 81.6 ($\text{C}(\text{CH}_3)_3$), 170.3 and 170.7 (CO). ^{29}Si NMR (CDCl_3): δ 1.6 (SiMe), 2.0 ($\text{SiCH}_2\text{CH}_2\text{S}$). Anal. Calcd for $\text{C}_{63}\text{H}_{134}\text{N}_8\text{O}_6\text{S}_4\text{Si}_3\text{NaCl}$ (1312.30 g/mol): C, 55.15; H, 9.77; N, 8.17; S, 9.33. Found: C, 54.70; H, 8.78; N, 7.45; S, 8.39. MS: $[\text{M} + \text{H}]^+ = 1311.77$ uma (calcd = 1311.86 uma).

Synthesis of $\text{DO3AG}_1(\text{NMe}_2)_2$ (17**).** To a solution of compound **15** (0.200 g, 0.228 mmol) in methanol was added dropwise an aqueous solution of NaOH (2 mL, 0.082 g, 2.05 mmol). The reaction mixture was stirred for 1 h at room temperature. The residue was purified by size exclusion chromatography in water (Sephadex), which gave the compound **17** as a yellow oil (0.100 g, 57% yield). ^1H NMR (MeOD): δ 0.01 (s, 3 H, SiMe), 0.48 (m, 2 H, CH_2Si), 0.79 (t, 4 H, $\text{SiCH}_2\text{CH}_2\text{S}$), 1.21 (m, 2 H, $\text{CH}_2\text{CH}_2\text{Si}$), 1.53 (m, 2 H, NCH_2CH_2), 1.90–3.80 (m, 24 H, $\text{N}(\text{CH}_2)_2\text{N}$, NCH_2 , and NCH_2COO), 2.17 (s, 12 H, $\text{SCH}_2\text{CH}_2\text{NMe}_2$), 2.32–2.81 (m, 4 H, $\text{SCH}_2\text{CH}_2\text{NMe}_2$, 4 H, $\text{SiCH}_2\text{CH}_2\text{S}$, 4 H, $\text{SCH}_2\text{CH}_2\text{NMe}_2$). $^{13}\text{C}\{^1\text{H}\}$ NMR (MeOD): δ –5.2 (MeSi), 13.1 (SiCH_2), 14.5 ($\text{SiCH}_2\text{CH}_2\text{S}$), 21.1 ($\text{NCH}_2\text{CH}_2\text{CH}_2\text{CH}_2\text{Si}$), 29.6 ($\text{SiCH}_2\text{CH}_2\text{S}$), 36.8 ($\text{NCH}_2\text{CH}_2\text{CH}_2\text{CH}_2\text{Si}$), 45.15–51.19 ($\text{N}(\text{CH}_2)_2\text{N}$), 44.1 ($\text{SCH}_2\text{CH}_2\text{NMe}_2$), 51.8 ($\text{SCH}_2\text{CH}_2\text{NMe}_2$), 58.8 ($\text{SCH}_2\text{CH}_2\text{NMe}_2$), 170.5 (COONa). ^{29}Si NMR (MeOD): δ –2.2 ($\text{SiCH}_2\text{CH}_2\text{S}$). Anal. Calcd for $\text{C}_{31}\text{H}_{64}\text{Cl}_3\text{N}_6\text{Na}_3\text{O}_6\text{S}_2\text{Si}$ (884.42 g/mol): C, 42.10; H, 7.29; N, 9.50; S, 7.25. Found: C, 41.88; H, 7.12; N, 9.40; S, 6.89.

Synthesis of $\text{DO3AG}_2(\text{NMe}_2)_4$ (18**).** The reaction of compound **16** (0.160 g, 0.122 mmol) with NaOH (2 mL, 0.043 g, 1.10 mmol) was carried out in a similar way to that for the synthesis of **17**. Compound **18** was obtained as a pale yellow solid (0.110 g, 75% yield). ^1H NMR (MeOD): δ 0.02 (s, 3 H, SiMe), 0.09 (s, 6 H, SiMe), 0.57 (m, 10 H, SiCH_2), 0.86 (t, 8 H, $\text{SiCH}_2\text{CH}_2\text{S}$), 1.44 (m, 8 H, $\text{CH}_2\text{CH}_2\text{Si}$ and NCH_2CH_2), 1.90–3.70 (m, 24 H, $\text{N}(\text{CH}_2)_2\text{N}$, NCH_2COO , and NCH_2CH_2), 2.20 (s, 24 H, $\text{SCH}_2\text{CH}_2\text{NMe}_2$), 2.53–2.71 (m, 8 H, $\text{SCH}_2\text{CH}_2\text{NMe}_2$, 8 H, $\text{SiCH}_2\text{CH}_2\text{S}$, 8 H, $\text{SCH}_2\text{CH}_2\text{NMe}_2$). $^{13}\text{C}\{^1\text{H}\}$ NMR (MeOD): δ –5.1 and 5.2 (MeSi), 16.7 ($\text{SiCH}_2\text{CH}_2\text{S}$), 20.9 (CH_2), 28.2 ($\text{SiCH}_2\text{CH}_2\text{S}$), 43.7 ($\text{SCH}_2\text{CH}_2\text{NMe}_2$), 51.7 ($\text{SCH}_2\text{CH}_2\text{NMe}_2$), 58.8 ($\text{SCH}_2\text{CH}_2\text{NMe}_2$), 175.8 (COO). ^{29}Si NMR (MeOD): δ 1.63 (SiMe), 2.06 ($\text{SiCH}_2\text{CH}_2\text{S}$). Anal. Calcd for $\text{C}_{51}\text{H}_{112}\text{Cl}_3\text{N}_8\text{Na}_2\text{O}_6\text{S}_4\text{Si}_3$ (1262.89 g/mol): C, 45.93; H, 8.46; N, 8.40; S, 9.62. Found: C, 44.57; H, 8.10; N, 8.45; S, 8.62.

■ ASSOCIATED CONTENT

● Supporting Information

The Supporting Information is available free of charge on the ACS Publications website at DOI: 10.1021/acs.inorgchem.5b01047.

^1H and ^{13}C NMR, UV–vis, and EPR spectra and potentiometric titration of selected compounds (PDF)

■ AUTHOR INFORMATION

Corresponding Authors

*Tel (F. Ottaviani): (+39) 0722 304320. Fax: (+39) 0722 304222 E-mail: maria.ottaviani@uniurb.it.

*Tel (R. Gómez): (+34) 91 8854685. Fax: (+34) 91 8854683. E-mail: rafael.gomez@uah.es.

Notes

The authors declare no competing financial interest.

■ ACKNOWLEDGMENTS

This work has been supported by grants from MINECO CTQ2011-23245 and CTQ2014-54004-P, Consortium NANODENDMED ref S2011/BMD-2351 (CAM), and also CIBER-BBN as an initiative funded by the VI National R & D & i Plan 2008-2011, Iniciativa Ingenio 2010, Consolider

Program, CIBER Actions and financed by the Instituto de Salud Carlos III, with assistance from the European Regional Development Fund. M.F.O. acknowledges financial support from PRIN2012–NANOMed. COST Action MP1202 is also acknowledged for supporting visit exchanges.

REFERENCES

- (1) Gaynor, D.; Griffith, D. M. *Dalton Trans.* **2012**, 41, 13239–13257.
- (2) *Bioinorganic Medicinal Chemistry*; Alessio, E., Ed.; Wiley-VCH: Weinheim, Germany, 2011.
- (3) Wadas, T. J.; Wong, E. H.; Weisman, G. R.; Anderson, C. J. *Chem. Rev.* **2010**, 110, 2858–2902.
- (4) De León-Rodríguez, L. M.; Kovacs, Z. *Bioconjugate Chem.* **2008**, 19, 391–402.
- (5) Vorakova, I.; Venek, J.; Pasulka, J.; Strelcova, Z.; Lubal, P.; Hermann, P. *Polyhedron* **2013**, 61, 99–104.
- (6) Barge, A.; Tei, L.; Upadhyaya, D.; Fedeli, F.; Beltrami, L.; Stefania, R.; Aime, S.; Cravotto, G. *Org. Biomol. Chem.* **2008**, 6, 1176–1178.
- (7) Calce, E.; Monfregola, L.; De Luca, S. *Int. J. Pept. Res. Ther.* **2013**, 19, 199–202.
- (8) Jamous, M.; Haberkorn, U.; Mier, W. *Tetrahedron Lett.* **2012**, 53, 6810–6814.
- (9) Kepp, K. P. *Chem. Rev.* **2012**, 112, 5193–5239.
- (10) Hamley, I. W. *Chem. Rev.* **2012**, 112, 5147–5192.
- (11) Svenson, S.; Tomalia, D. *Adv. Drug Delivery Rev.* **2005**, 57, 2106.
- (12) Menjoge, A. R.; Kannan, R. M.; Tomalia, D. A. *Drug Discovery Today* **2010**, 15, 171.
- (13) Medina, S. H.; El-Sayed, M. E. H. *Chem. Rev.* **2009**, 109, 3141.
- (14) Mintzer, M. A.; Simanek, E. E. *Chem. Rev.* **2009**, 109, 259–302.
- (15) Liu, X.; Rocchi, P.; Peng, L. *New J. Chem.* **2012**, 36, 256–263.
- (16) Heegaard, P. M. H.; Boas, U.; Sorensen, N. S. *Bioconjugate Chem.* **2010**, 21, 405–418.
- (17) Shcharbin, D. G.; Klajnert, B.; Bryszewska, M. *Biochemistry* **2009**, 48, 1070–1079.
- (18) Mintzer, M. A.; Dane, E. L.; O'Toole, G. A.; Grinstaff, M. W. *Mol. Pharmaceutics* **2012**, 9, 342–354.
- (19) Chen, C. Z.; Beck-Tan, N. C.; Dhurjati, P.; van Dyk, T. K.; LaRossa, R. A.; Cooper, S. L. *Biomacromolecules* **2000**, 1, 473–480.
- (20) Rasines, B.; Hernández-Ros, J. M.; de las Cuevas, N.; Copa-Patiño, J. L.; Soliveri, J.; Muñoz-Fernández, M. A.; Gómez, R.; de la Mata, F. J. *Dalton Trans.* **2009**, 8704–8713.
- (21) McCarthy, J. M.; Appelhans, D.; Tatzelt, J.; Rogers, M. S. *Prion* **2013**, 7, 198–202.
- (22) Benseny-Cases, N.; Klementieva, O.; Cladera, J. *New J. Chem.* **2012**, 36, 211–216.
- (23) Rolland, O.; Turrin, C.-O.; Caminade, A.-M.; Majoral, J.-P. *New J. Chem.* **2009**, 33, 1809–1824.
- (24) Galán, M.; Rodríguez, J. S.; Jiménez, J. J.; Relloso, M.; Maly, M.; de la Mata, F. J.; Muñoz-Fernández, M. A.; Gomez, R. *Org. Biomol. Chem.* **2014**, 12, 3222–3237.
- (25) Vacas-Córdoba, E.; Arnaiz, E.; Relloso, M.; Sanchez-Torres, C.; García, F.; Perez-Alvarez, L.; Gomez, R.; de la Mata, F. J.; Pion, M.; Muñoz-Fernández, M. A. *AIDS* **2013**, 27, 1219–1229.
- (26) Longmire, M.; Choyke, P. L.; Kobayashi, H. *Curr. Top. Med. Chem.* **2008**, 8, 1180–1186.
- (27) Fernandez-Trillo, F.; Pacheco-Torres, J.; Correa, J.; Ballesteros, P.; Lopez-Larrubia, P.; Cerdán, S.; Riguera, R.; Fernández-Megía, E. *Biomacromolecules* **2011**, 12, 2902–2907.
- (28) Tomalia, D. A.; Christensen, J. B.; Boas, U. *Dendrimers, Dendrons and Dendritic Polymers*; Cambridge University Press, 2012.
- (29) Dijkgraaf, I.; Rijnders, A. Y.; Soede, A.; Dechesne, A. C.; van Esse, G. W.; Brouwer, A. J.; Corstens, F. H. M.; Boerman, O. C.; Rijkers, D. T. S.; Liskamp, R. M. J. *Org. Biomol. Chem.* **2007**, 5, 935–944.
- (30) Jiménez, J. L.; Pion, M.; de la Mata, F. J.; Gómez, R.; Muñoz, E.; Leal, M.; Muñoz-Fernández, M. A. *New J. Chem.* **2012**, 36, 299–309.
- (31) Fuentes, E.; Hernandez-Ros, J. M.; Sanchez-Milla, M.; Camero, M. A.; Maly, M.; Perez-Serrano, J.; Copa-Patino, J. L.; Sanchez-Nieves, J.; Soliveri, J.; Gómez, R.; Javier de la Mata, F. *RSC Adv.* **2014**, 4, 1256–1265.
- (32) Vacas-Córdoba, E.; Arnaiz, E.; de la Mata, F. J.; Gómez, R.; Leal, M.; Pion, M.; Muñoz-Fernández, M. A. *AIDS* **2013**, 27, 2053–2058.
- (33) Fuentes, E.; Peña-González, C. E.; Galán, M.; Gómez, R.; de la Mata, F. J.; Sánchez-Nieves, J. *Organometallics* **2013**, 32, 1789–1796.
- (34) Galán, M.; Fuentes, E.; de la Mata, F. J.; Gómez, R. *Organometallics* **2014**, 33, 3977–3989.
- (35) García-Gallego, S.; Rodríguez, J. S.; Jiménez, J. L.; Cangiotti, M.; Ottaviani, M. F.; Muñoz-Fernández, M. A.; Gómez, R.; de la Mata, F. J. *Dalton Transaction* **2012**, 41, 6488–6499.
- (36) García-Gallego, S.; Cangiotti, M.; Fiorani, L.; Fattori, A.; Muñoz-Fernández, M. A.; Gomez, R.; Ottaviani, M. F.; de la Mata, F. J. *Dalton Trans.* **2013**, 42, 5874–5889.
- (37) Ottaviani, M. F.; Bossmann, S.; Turro, N. J.; Tomalia, D. A. *J. Am. Chem. Soc.* **1994**, 116, 661–671.
- (38) Ottaviani, M. F.; Cangiotti, M.; Fattori, A.; Coppola, C.; Lucchi, S.; Ficker, M.; Petersen, J. F.; Christensen, J. B. *J. Phys. Chem. B* **2013**, 117, 14163–14172.
- (39) Ottaviani, M. F.; Cangiotti, M.; Fattori, A.; Coppola, C.; Posocco, P.; Laurini, E.; Liu, X.; Liu, C.; Fermeleglia, M.; Peng, L.; Prich, S. *Phys. Chem. Chem. Phys.* **2014**, 16, 685–694.
- (40) Sevcik, R.; Vanek, J.; Lubal, P.; Kotkova, Z.; Kotek, J.; Hermann, P. *Polyhedron* **2014**, 67, 449–455.
- (41) For theoretical potentiometric data, the programs Marvin, Calculator Plugin, and Chemiscal Terms Demo were used.
- (42) Van Duijvenbode, R. C.; Rajanayagam, A.; Koper, G. J. M.; Baars, M. W. P. L.; de Waal, B. F. M.; Meijer, E. W.; Borkovec, M. *Macromolecules* **2000**, 33, 46–52.
- (43) Hathaway, B. J.; Dudley, R. J.; Nicholls, P. *J. Chem. Soc. A* **1969**, 1845–1848.
- (44) Hathaway, B. J.; Procter, I. M.; Slade, R. C.; Tomlinson, A. A. *J. Chem. Soc. A* **1969**, 2219–2224.
- (45) Kurosaki, H.; Koike, H.; Omori, S.; Ogata, Y.; Yamaguchi, Y.; Goto, M. *Inorg. Chem. Commun.* **2004**, 7, 1229–1232.
- (46) Kurdziel, K.; Glowinski, T. *Polyhedron* **2000**, 19, 2183–2188.
- (47) Papish, E. T.; Taylor, M. T.; Jernigan, F. E.; Rodig, M. J.; Shawhan, R. R.; Yap, G. P. A.; Jove, F. A. *Inorg. Chem.* **2006**, 45, 2242–2250.
- (48) Prenesti, E.; Daniele, P. G.; Berto, S.; Toso, S. *Polyhedron* **2006**, 25, 2815–2823.
- (49) Leong, W. L.; Vittal, J. J. *J. Inclusion Phenom. Mol. Recognit. Chem.* **2011**, 71, 557–566.
- (50) Budil, D. E.; Lee, S.; Saxena, S.; Freed, J. H. *J. Magn. Reson., Ser. A* **1996**, 120, 155–189.
- (51) Davis, F. J.; Gilbert, B. C.; Norman, R. O. C.; Symons, M. C. R. *J. Chem. Soc., Perkin Trans. 2* **1983**, 2, 1763–1771.
- (52) Xie, Y.; Riedinger, A.; Prato, M.; Casu, A.; Genovese, A.; Guardia, P.; Sottini, S.; Sangregorio, C.; Misztal, K.; Ghosh, S.; Pellegrino, T.; Manna, L. *J. Am. Chem. Soc.* **2013**, 135, 17630–17637.
- (53) Addison, A. W. In *Copper Coordination Chemistry: Bio-chemical and Inorganic Perspectives*; Karlin, K. D.; Zubieta, J., Eds.; Adenine Press: Guilderland, NY, 1983; p 109.
- (54) Solomon, E. I.; Hanson, M. A. In *Inorganic Electronic Structure and Spectroscopy, Vol. II: Applications and Case Studies*; Solomon, E. I.; Lever, A. B. P., Eds.; John Wiley & Sons: New York, 2006; p 1.
- (55) Ogawa, T.; Shimoi, M.; Ouchi, O. *Bull. Chem. Soc. Jpn.* **1982**, 55, 126–129.
- (56) Kneubuhl, F. K. *J. Chem. Phys.* **1960**, 33, 1074–8.
- (57) Riesen, A.; Zehnder, M.; Kaden, T. A. *Helv. Chim. Acta* **1986**, 69, 2067–2073.